

Characterisation of Hippocampal Sclerosis and the Assessment of the Kynurenic Acid Analogue SZR104 in a Murine Model of Pilocarpine-induced Epilepsy

Ph.D. Thesis

Adrienne Mátyás, M.Sc.

Supervisor:

András Mihály, M.D., Ph.D., D.Sc.

Professor Emeritus

Doctoral School of Theoretical Medicine, University of Szeged, Hungary

Albert Szent-Györgyi Medical School, University of Szeged, Hungary

Department of Anatomy, Histology and Embryology

Szeged

2024

I dedicate this thesis to my parents, my husband, and my daughters.

List of publications (cumulative IF: 18.849)

Publications related to the subject of the thesis (cumulative IF: 11.524)

- I. **Mátyás A**, Borbély E, Mihály A. Hippocampal Sclerosis in Pilocarpine Epilepsy: Survival of Peptide-Containing Neurons and Learning and Memory Disturbances in the Adult NMRI Strain Mouse. **Int J Mol Sci.** 2022; 23 (1):204. 19 p. (IF (2022): 5.6, SJR: Q1)
- II. Lajkó N, Kata D, Szabó M, **Mátyás A**, Dulka K, Földesi I, Fülöp F, Gulya K, Vécsei L, Mihály A. Sensitivity of Rodent Microglia to Kynurenines in Models of Epilepsy and Inflammation In Vivo and In Vitro: Microglia Activation is Inhibited by Kynurenic Acid and the Synthetic Analogue SZR104. **Int J Mol Sci.** 2020; 21 (23):9333. 15 p. (IF (2020): 5.924, SJR: Q1)

Publications not included in the thesis (cumulative IF: 7.325)

- I. Toth Z, Mihaly A, **Matyas A**, Krisztin-Peva B. Non-competitive antagonists of NMDA and AMPA receptors decrease seizure-induced c-fos protein expression in the cerebellum and protect against seizure symptoms in adult rats. **Acta Histochemica** 2018; 120:3 pp. 236-241; 6 p. (**IF (2018): 1.719**, SJR: **Q2**)
- II. Kovács T, Lootz K, Dorn Á, Andrieu J, Horváth M, **Mátyás A**, Schneider Gy. Potential of small-scale jar systems to extend the shelf life of raw meats, and hinder the proliferation of *Campylobacter jejuni* and Enterohemorrhagic *Escherichia coli*. **LWT-Food Science And Technology** 2017; 79 pp. 525-533; 9 p. (**IF (2017): 3.129**, SJR: **D1**)
- III. Farkas E, Sule Z, Toth-Szuki V, **Matyas A**, Antal P, Farkas IG, Mihaly A, Bari F. Tumor necrosis factor-alpha increases cerebral blood flow and ultrastructural capillary damage through the release of nitric oxide in the rat brain. **Microvascular Research** 2006; 72: 3 pp. 113-119; 7 p. (**IF (2006): 2.477**, SJR: **Q1**)

Table of contents

List of publications	II
Abbreviations	VI
1. Introduction	1
1.1. Definition of epilepsy	2
1.2. Epidemiology of epilepsy	2
1.3. Aetiology of epilepsy	3
1.4. Classification of epilepsies	4
1.5. Pathogenesis and pathology of TLE	4
1.6. Anatomy and fine structure of the hippocampus	5
1.7. Characterisation of hippocampal sclerosis associated with MTLE	9
1.8. Preclinical MTLE models	10
1.9. Status epilepticus	11
1.10. The murine model of pilocarpine-induced epilepsy	11
1.11. Measure of spatial learning and memory	13
1.12. Potential neuroprotective effect of kynurenic acid and its synthetic analogue SZR104 in preclinical epilepsy models	14
2. Aims	16
3. Materials and Methods	17
3.1. Experimental protocol and pharmacological treatment	17
3.2. Tissue preparation	19
3.3. Immunohistochemistry	19
3.4. Spatial learning test using the Barnes maze	20
3.5. Morphometry and evaluation of data	21
4. Results	23
4.1. Neuronal loss and shrinkage of the hippocampus 3.5 months after SE	23
4.2. Microglial activation and proliferation 3.5 months after SE in HF	27
4.3. Sprouting of mossy fibres 3.5 months after SE	27
4.4. Parvalbumin -containing hippocampal interneurons 3.5 months after SE	28
4.5. Alterations in the number of CALR-immunostained cells	30
4.6. The impairment of spatial learning 3 months after SE	32
4.7. A case report in pilocarpine-induced NMRI-strain epileptic mice	33
4.8. Effect of SZR104 on hippocampal microglial cells in pilocarpine-induced epileptic mice	34

5. Discussion	36
5.1. Learning and memory impairment caused by severe HS in epileptic mice	37
5.2. Neuronal loss, microglial activation, and sprouting of mossy fibres in epileptic mice	37
5.3. Specific loss of PARV-immunopositive and CALR-immunopositive interneurons in epileptic mice	40
5.4. SZR104 effect on changes in number and phenotype of microglial cells in pilocarpine-induced epileptic mice	43
6. Conclusions	44
Acknowledgements	45
Bibliography	46
Co-Authors' statement	
Appendix	

Abbreviations

ANOVA	analysis of variance
AOI	area of interest
BBB	blood - brain barrier
BrdU	thymidine analog 5'-bromo-2'-deoxyuridine
bwt	body weight
CA	<i>cornu ammonis</i> (Ammon's horn)
CALB	calbindin
CALR	calretinin
CALR-IR	calretinin immunoreactive
CNS	central nervous system
DAM	disease-associated microglia
DG	dentate gyrus
EB	escape box
f / Fim	fimbria
Fis	hippocampal fissure
GC	granule cell
HF	hippocampal formation
HS	hippocampal sclerosis
Iba1	ionized calcium binding adaptor molecule 1
IHC	immunohistochemistry
IL-6	interleukin-6
IML	internal molecular layer
i.p.	intraperitoneally
IR	immunoreactive
KYNA	kynurenic acid
MC	mossy cell
MRI	magnetic resonance imaging
MTLE	medial temporal lobe epilepsy
NeuN	neuronal nuclear protein
Neuro D	neuronal mouse monoclonal IgG ₁
NMDA	N - methyl - D - aspartic acid
NMRI	Naval Medical Research Institute (inbred albino mouse line)

NPY	neuropeptide-Y
PARV	parvalbumin
PILO	pilocarpine-treated
PC	pyramidal cell
RT	room temperature
SE	status epilepticus
SEM	standard error of the mean
SRS	spontaneous recurrent seizures
SZR104	N-(2-(dimethyl amino) ethyl)-3-(morpholinomethyl)-4-hydroxyquinoline- 2-carboxamide
TLE	temporal lobe epilepsy

1. Introduction

Epilepsy is a chronic, noninfectious brain disease that affects people of all ages worldwide. In total, 50 million people were diagnosed with epilepsy in 2020, almost 80% of them living in developing countries [1].

As a disease, epilepsy is a complex social and economic problem. Living with epilepsy can not only be a challenge for patients and their families, but also put a great burden on the neurological and paediatric health care systems. However, with appropriate medical care, support, and management strategies, many people with epilepsy can lead a full and productive life. An estimated 70% of patients with epilepsy could be seizure-free if properly diagnosed and treated. However, about three-quarters of people with epilepsy in low-income countries do not receive the treatment they need, and this can reach 90%. In these countries, many health professionals do not have training to recognise, diagnose, and treat epilepsy. In the most resource-poor countries, antiepileptic drugs are not available. The WHO is working with the ministries of health and its partners to improve access to affordable epilepsy treatment [1].

In the European Union alone, the pharmaceutical industry has a market of € 20 billion to treat the disease, yet a third of patients are ineffective.

The economic, social and personal burden of this disorder underscores the need for more research efforts that lead to new approaches for the diagnosis, treatment, and prevention of epilepsy and its consequences. There are two main pillars of these research efforts: on the one hand, researchers are focusing on how to reduce seizure activity and minimize its impact on life quality; on the other hand, more forward-looking experiments are being conducted targeting the prevention of convulsions. This preventive approach can also be achieved through pharmacotherapy, but there are many attempts to develop more targeted and less expensive therapeutic instruments to prevent seizures. Although human studies would be optimal, they are not always possible or feasible due to obvious ethical, statistical, and financial constraints. Consequently, preclinical studies employing animal models to study and test new therapeutic mechanisms remain important and indispensable.

In the subsequent sections of the Introduction, I will first briefly review the nomenclature, epidemiology, and clinical classification of epilepsy syndromes, then focus on the neuropathology and pathophysiology of temporal lobe epilepsy (TLE) and how it can be studied in experimental animal models.

1.1. Definition of epilepsy

Epileptic syndromes are one of the most common neurological diseases, characterised by a tendency to have recurrent unprovoked seizures. More appropriately, epilepsies are now regarded a group of conditions with different pathophysiologies, aetiologies, and various manifestations depending on factors such as the part of the brain affected, the individual's age, the underlying causes, and the spread of seizure activity.

Seizures and epilepsy are complex neurological conditions that arise from the hyperexcitability of neurons in the cerebral hemispheres. Abnormal electrical activity in the brain can cause seizures that can recur, often spontaneously and without warning.

Physiologically, epilepsy is characterised by occasional sudden, excessive, rapid, and local discharges of cortical neurons. Current evidence suggests that increased and hypersynchronous neuronal discharges play a critical role in the generation of seizures.

On a clinical level, epileptic seizures are intermittent events that typically onset suddenly, spread rapidly, and are usually brief [2-4].

Uncontrolled electrical disturbances in the brain can manifest as a variety of symptoms, including involuntary movements, sensory disturbances, changes in behaviour or feelings, loss of consciousness, and autonomic changes. Seizures can be preceded by a prodrome, may include an aura, and can be followed by a postictal state. The abnormal cerebral electrical activity (hyperactivity) during seizures can be detected and analysed by electroencephalography (EEG) [5] and magnetic resonance imaging (MRI) [6].

1.2. Epidemiology of epilepsy

After stroke, epilepsy has become the second most common neurological disease worldwide. Regarding geographical differences, national and international surveys have not shown significant variations in the global prevalence of epilepsy. It can affect individuals of any race, age, or social class. However, individuals with a family history of epilepsy may have a slightly higher risk compared to the general population. Although epilepsy can develop at any stage of life, it is more common in elderly people. There are two peak prevalence periods: infancy and childhood and older than 60 - 70 years.

In Hungary, epilepsy affects 0.3 - 0.6% of the population, that is, about 30 - 60 thousand people diagnosed with epilepsy in 2010 [7].

The incidence of the disease is 0.4 to 1%. This value is highest in childhood and infancy, when it exceeds 1%, with a decreasing trend from infancy to adolescence. Due to epilepsy that often lasts for decades, the cumulative incidence can reach 3 to 5% at the end of life [8].

1.3. Aetiology of epilepsy

Epileptic seizures are complex events that involve abnormal excitability and synchronisation of neuronal activity in the brain. There is often a cycle of excitation followed by inhibition and subsequent rebound excitation, leading to synchronised firing of neurons and the generation of seizure activity. Altered neuronal membrane permeability and disturbances in the regulation of extracellular ion concentrations lead to membrane depolarisation and alteration of the spatial and temporal distribution of excitatory and inhibitory synapses. All of this affects the excitatory postsynaptic potential (EPSP) / inhibitory postsynaptic potential (IPSP) ratio, damage to receptors in postsynaptic membranes, and imbalance between excitatory and inhibitory neurotransmitters. Finally, all of these together contribute to increased neuronal excitability and can play a role in the development of seizures [9].

Abnormal stimulation through specific pathways and reverberation through excitatory recurrent pathways can trigger spasms and cause significant destruction of the sensitive neuronal cell population [10].

The combined abnormal interaction between the excitatory and inhibitory systems is crucial in the generation and termination of epileptic seizures. The coordinated action of the feedback and feedforward functions of inhibitory neurons helps regulate neuronal activity and can influence the occurrence of seizures. Several excitatory cells are simultaneously inhibited, and then, after the refractory phase, these neurons are able to trigger an action potential simultaneously [9].

The range of potential causes of epilepsy varies with age. In infants, common acquired causes include perinatal hypoxia/asphyxia, perinatal intracranial trauma, metabolic disturbances, congenital malformations of the brain, and infections that can cause generalised seizures. In young children and adolescents, idiopathic (genetically determined) epilepsies are prevalent. In adults, there is an equal prevalence of focal and generalised seizures, typically due to tumour, alcoholism, cerebrovascular disorders, or neurotrauma [2, 3, 11]. Adult-onset epilepsy can result from causes that originated in childhood, but in young adults, factors such as alcohol consumption and head injuries are among the common triggers. In elderly people, the prevalence is skewed toward focal seizures and brain tumours account for a significant proportion of epilepsy cases in people between the ages of 30 and 50, while cerebrovascular disease becomes the leading cause in those over 50 years of age. There is growing evidence of a link between Alzheimer's disease and epilepsy. Epilepsy and epileptiform activity in old age can precede the cognitive decline characteristic of Alzheimer's disease by years, and the presence of seizures has been shown to predict a more rapid progression of the disease [12].

Understanding the complex interplay of excitatory and inhibitory systems in the brain is essential to develop effective treatments for epilepsy and to manage seizures in affected individuals.

1.4. Classification of epilepsies

The classification of seizures is fairly complex. However, two main groups are widely accepted, based on EEG. In focal epilepsy, the seizure originates in a limited area of the brain (ictus) and causes slightly milder symptoms, whereas in generalised epilepsy the seizure appears in the entire cortex at the same time [13].

Depending on the underlying cause, we can differentiate genuine epilepsy from symptomatic epilepsy. Although genuine epilepsy is idiopathic and structural cerebral lesions can not be demonstrated, symptomatic epilepsies can be caused by acquired CNS injuries or congenital abnormalities. Temporal lobe epilepsy (TLE) corresponds to complex partial epilepsy according to the officially adopted classification based on the recommendation of the International League Against Epilepsy (ILAE) [14].

1.5. Pathogenesis and pathology of TLE

There are no clear data on the prevalence of TLE, but it is likely to account for 50 - 70% of adult epilepsies, making it the most common type of epilepsies [3].

The term TLE refers to the epileptogenic focus. A finer distinction is made between lateral and medial TLE with respect to a more precise location of the trigger site. Temporolateral epilepsy (neocortical) is more common in childhood, whereas mediotemporal epilepsy (MTLE) is found mainly in adults [15]. Most patients with MTLE already have the initial triggers (hypoxia, trauma, intracranial infections, febrile convulsions) that may be responsible for the development of the disease before the age of five. Among these, febrile convulsions should be highlighted, as they are present in the anamnesis of almost 60% of MTLE with hippocampal sclerosis [16]. Several studies have reported that febrile convulsions can cause MTLE [17, 18], while others have not found a direct association between febrile conditions and epilepsy. Therefore, it can be concluded that the association between epilepsy and febrile convulsions is indirect and the role of genetic factors in epileptogenesis can not be ignored [19]. The febrile convulsions in infancy can rarely be followed by the first epileptic seizures - mainly tonic-clonic seizures in late childhood. The frequency of seizures is reduced in many cases or even eliminated because early therapy increases the threshold for seizures. However, with puberty, the frequency of complex partial seizures increases and unfortunately shows little or no

response to antiepileptic drugs. The persistence of epilepsy into adulthood fluctuates depending on the treatments used.

Surgery can be a successful and definitive solution in 80 - 85% of cases, if the epileptogenic focus is well defined [20]. However, most patients have access to surgery too late and rehabilitation is often insufficient, which otherwise would be essential for functional recovery. Psychopathological complications are not uncommon, such as affective disorders (depression), cognitive deficits, etc. The accepted hypothesis of the pathogenesis of MTLE involves the following three main steps [3]:

- 1) In childhood, a damaging epileptogenic factor hits the hippocampus, which is genetically and structurally very sensitive. At this stage, there is significant neuronal loss in the most sensitive hippocampal regions, such as the pyramidal cells (PC) of CA3.
- 2) During the latent period, the time required for the MTLE morphology to develop, gliosis occurs accompanied by synaptic reorganisation of the hippocampus [21]. This alteration is also confirmed in humans, because such a sclerotised hippocampus, and especially as a consequence the more dilated inferior horn of the lateral ventricle can be visualised on magnetic resonance imaging (MRI).
- 3) Complex partial seizures develop, which unfortunately become less and less treatable with epileptic drugs over time and thus become therapy resistant.

Even under physiological conditions, the hippocampus undergoes significant development and maturation during postnatal ontogenesis. The first week after birth is a critical time window compared to the subsequent weeks. Probably the rapid changes of the hippocampus during this critical developmental window may make it vulnerable to the initial triggers that can ultimately lead to MTLE. Two prominent hippocampal cell types play a primary role in this process: PC and the granule cell (GC). Mature PCs have already developed in the hippocampus at birth, whereas GCs mature only about two weeks later [22]. GCs are among the most vulnerable sets of neurons to seizure-induced neurodegeneration in adult-onset epilepsy. Therefore, GC lesions may contribute more to epileptogenesis compared to PCs in adults. This is in agreement with the observations that lesions occur early in postnatal life are less epileptogenic than later ones [23].

1.6. Anatomy and the fine structure of the hippocampus

The previous section highlighted the exquisite role that hippocampal neurons play in the pathomechanism of MTLE, one of the most common forms of epilepsy. Their involvement has been confirmed by several human studies detailing the neuropathological changes in the

hippocampus [24, 25]. Therefore, detailed knowledge of the morphology and neuronal networks of this limbic structure is warranted to correctly describe the changes associated with epilepsy. The term ‘hippocampus’ *per se*, which is central to MTLE pathogenesis, needs some clarification. The structure involved is properly called the hippocampal complex or hippocampal formation (HF) consists of the subiculum, the hippocampus proper / Ammon’s horn / *cornu ammonis* (CA), and the dentate gyrus (DG) (Figure 1). The HF maintains reciprocal connections with almost all sensory and association areas of the brain through the entorhinal cortex [26-28]. The DG is a thin gyrus deep in the hippocampal sulcus. Its surface is slightly serrated, hence the name. The CA is further divided into four parts and corresponding to the abbreviations they are termed as CA1, CA2, CA3, and CA4 regions.

Based on their cytoarchitectonic features, there are two types of cerebral cortex: the allocortex (also termed heterogenic cortex) and the neocortex (known as the isocortex). In humans, the allocortex comprises only approximately 10% of the cortical mass [29]. The further division of the allocortex is as follows: paleocortex, archicortex, and a transitional zone between the neocortex and the allocortex, termed periallocortex [30]. By the currently accepted nomenclature, the main areas of the archicortex are the CA and the DG. The allocortex is characterised by having fewer cortical layers in contrast to the six-layered neocortex (Figure 1). However, the molecular layer of CA is divided into sublayers [31, 32]. The HF is a well-characterised and investigable brain area because its cellular organisation is spatially segregated, making it an excellent site for the cellular study of neuronal processes [33].

The principal neurons are arranged in a single layer: *stratum pyramidale* in CA and *stratum granulosum* in DG. Thus, the dendritic sections also form layers, and in addition, the recurrent collaterals of these cells also show laminarity. This arrangement can be observed in the afferents: fibres in the perforant pathway arising from the lateral entorhinal cortex terminate in the outer third of the *stratum moleculare* of DG, while the medial entorhinal cortex innervates the middle third [33, 34]. However, the inner third of the *stratum moleculare* is occupied by association and commissural fibres [33, 35]. The perforant pathway sends fibres directly to the *stratum lacunosum-moleculare* of CA1 and CA3, while the commissural and association fibres end together with the Schaffer collaterals in the *stratum oriens* and *stratum radiatum* [26, 27, 33, 36]. The *stratum moleculare* is a synaptic layer where the dendrites of PCs and the afferent commissural and association fibres synapse. Afferentation of the apical dendrites of PCs occurs in three layers: the most superficial layer of the *stratum moleculare* and the immediately underlying sublayer (*stratum lacunosum*) where the fibres from the ipsilateral entorhinal cortex terminate. The mossy fibres from the DG terminate in the sublayer closest to the cell bodies of

the PCs (*stratum radiatum*). The *stratum oriens* is also mainly a synaptic layer, although it contains scattered neurons. A similar layer in DG is called *stratum multiforme*, which is mentioned as the hilum in experimental animals, We have to note that there is no such thing in human official terminology. The alveus is the white matter of the subiculum and CA regions, immediately below the *stratum oriens*. The fimbria is the continuation of the confluent fibres of the alveus. However, it should be noted that not all the association fibres connecting hippocampal structures run in the alveus: The mossy fibres that run from the DG through the hilum to the apical dendrites of the PCs in CA3 form a separate sublayer, called the *stratum lucidum*. The afferents from the entorhinal cortex pass through the *stratum moleculare* to reach the apical dendrites of PCs and GCs, and the afferent pathway is called the perforant pathway. The regions of CA are connected by the Schaffer-collaterals. These also run in the *stratum moleculare* but innervate the distal part of the apical dendrites. The alveus contains the association fibres between the CA and the subiculum [37].

The perforant pathway is the most important excitatory pathway of the hippocampus, which contains three synapses. Its carried axons originate from the entorhinal cortex and run to the GCs of DG, where they synapse, and run as mossy fibres to PCs in CA3 to stimulate them. CA3 neurons innervate the PCs of the CA1 region through Schaffer collaterals. Furthermore, since CA3 neurons have an extensive excitatory collateral network and stimulate adjacent PCs, this explains the large number of neuronal synchronisations in epilepsy [9].

The main projection cells of the CA are the glutamatergic, stimulatory PCs in *stratum pyramidale*. These neurons are particularly vulnerable in epilepsy, mainly in the CA3 and CA1 regions. The CA1 region of the hippocampus is particularly vulnerable to hypoxic or ischemic damage and is known as Sommer's sector in the literature [38].

The main projecting cells of the DG are the glutamatergic, excitatory GCs, but these cells, unlike the previously mentioned ones, are resistant to even prolonged seizures. Glutamatergic neurons that stimulate association neurons in the hilum of the DG are the mossy cells (MC). The literature differs on the vulnerability to seizures of these cells. In contrast to Sloviter, whose conclusions are based on animal studies, it is revealed that the death of MCs leads to the development of subsequent recurrent seizures [39]. Scharfman's results support the concept, that these neurons can survive chronic seizures and even *status epilepticus* (SE) [40].

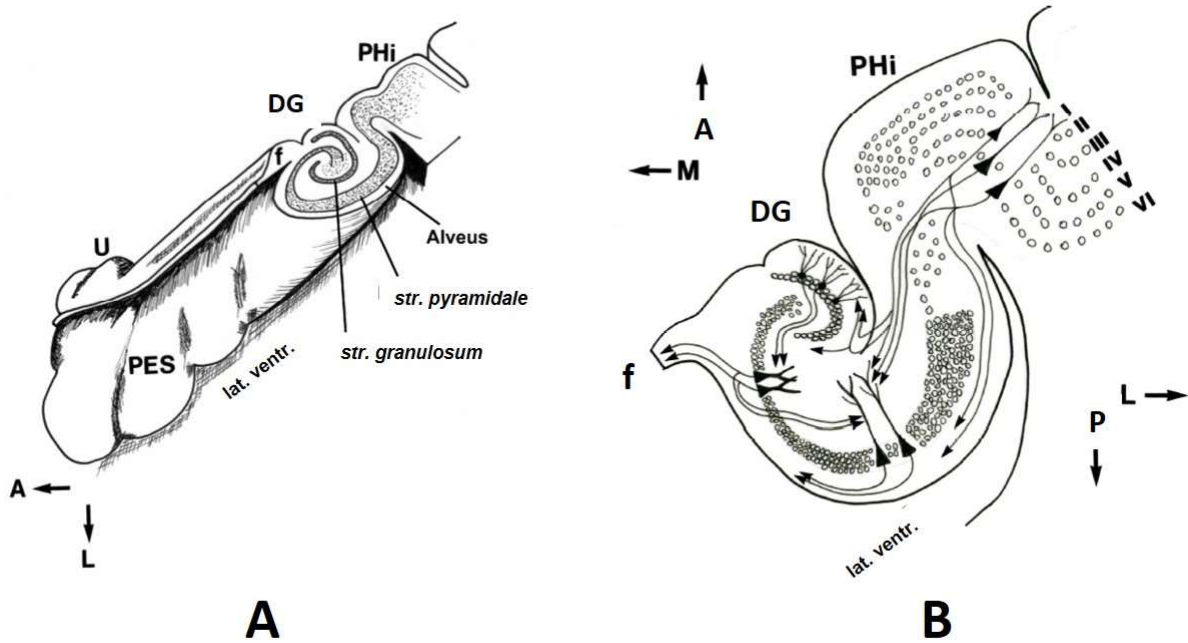


Figure 1. Schematic drawing of the surface of the hippocampus bulging into the lateral ventricle (A). Cross sectional part shows the cell layers of the principal neurons (*stratum pyramidale et granulosum*). (B) Schematic drawing of the hippocampal layers and neuronal network. The DG and CA, showing a simple layering characteristic, gradually transition to the six-layered parahippocampal gyrus (I-VI). Abbreviations: **DG** = dentate gyrus; **PHi** = parahippocampal gyrus; **U** = uncus; **f** = fimbria; **PES** = *pes hippocampi* [41].

In addition to the principal cells (PCs in CA and GCs in DG), and MCs, several types of inhibitory interneurons also reside in the hippocampus, thus, the function of the hippocampal neuronal network is highly dependent on the level and type of inhibition [42-47]. The main inhibitory transmitter is the gamma-aminobutyric acid (GABA), which is partially released from local inhibitory interneurons [48], or from nerve terminals of projecting axons of extrahippocampal origin [49-51]. Although local inhibitory GABAergic interneurons represent only ~10-15% of the total neuronal population in the hippocampus [52], their remarkable anatomical and physiological diversity still allows them to be the key determinants of local neuronal circuit activity and play a fundamental role in normal and pathological hippocampal function [53-56]. Epileptic discharge of principal cells may be caused by a reduction in inhibition below the normal level. [57-60]. These GABAergic cells determine the excitability of the principal cells and also affect certain subcortical afferent pathways [47, 51, 61, 62]. In the hippocampus, similar to most other CNS regions, the principal neurons are the most numerous, sharing many neurochemical and morphological properties. However, the interneurons to which they are connected are very diverse [33]. In addition to GABA, as the primary neurotransmitter, several other neuropeptides can be detected in these interneurons by

immunohistochemical techniques: enkephalins (Enk) [63], vasoactive intestinal polypeptide (VIP) [64, 65], cholecystokinin (CCK) [66-68], somatostatin (SOM) [68-71], neuropeptide-Y (NPY) [71]. Additional calcium-binding proteins are also present in a certain subpopulation of interneurons such as parvalbumin (PARV), calbindin (CALB) [56] and calretinin (CALR) [72-74].

1.7. Characterisation of hippocampal sclerosis associated with MTLE

Epileptic reorganisation refers to the following complex phenomena that involve neuroanatomical, physiological, and biochemical changes [75-78]:

- Changes affecting the whole nervous system (for example, modulation of EEG patterns, hormonal and metabolic changes).
- At the level of neuronal networks, intercellular connections are altered and axons die or sprout, leading to the death or sprouting of pathways, thus altering the connections between brain areas.
- At the cellular level, we can observe not only morphological changes [76] (e.g. cell swelling, increasing number of dendritic spines), cell death or division, migration, and gliosis, but also changes in neurochemical markers.
- Protein synthesis, receptors, and ion channels can be affected intracellularly [38].

There are three main types of axonal sprouting:

- Axonal sprouting of the local principal cells (= mossy fibre sprouting) is the most characteristic and the basis for the theoretical mechanism of MTLE [79].
- Sprouting of axons from external pathways (axons from the subiculum and supramammillary nucleus) [80, 81].
- Axonal sprouting of inhibitory interneurons [82].

All of these changes together lead to hippocampal sclerosis (HS), which is a condition characterised by shrinkage of the hippocampus and compensatory dilatation of the inferior horn of the lateral ventricle. Microscopically, this condition is often associated with extensive cell death in the CA1 and CA3 regions of the hippocampus, with some interneurons also affected, and gliosis is also observed [83].

There is a dilemma in the literature regarding HS, whether it is a cause or a consequence of epilepsy. Animal studies have shown that recurrent seizures can lead to the development of HS

[84]. It has been proven time and again that removal of the hippocampus can eliminate further seizures.

According to the criteria set by ILAE, the diagnosis of HS is usually based on the following characteristics [2, 3]:

- a. Clinical symptoms: Clinical symptoms in patients with epilepsy can include seizures, memory disturbances, and other neurological symptoms.
- b. Imaging tests: Brain imaging tests, such as MRI, can be used to detect changes in the hippocampus, such as shrinkage of the hippocampus and changes in the lateral ventricle. Extrahippocampal lesions of the limbic system can also develop (eg, amygdala, habenular nuclei, entorhinal cortex, central nuclei of the thalamus) [75, 85].
- c. Histological examinations: histological examinations can detect the minimum criteria for neuronal loss and gliosis, thickening of the granular cell layer, and other characteristic lesions at the microscopic level in different regions of the hippocampus. Synaptic reorganisation affects the mossy fibres and often also the supragranular layer of the DG.

These criteria can help diagnose HS and establish the treatment plan for affected patients. However, it is important to note that more clinical and imaging investigations may be needed to clarify the diagnosis and guide treatment, because the relationship between HS and epilepsy is complex and can vary among individuals.

1.8. Preclinical MTLE models

There are two main groups of animal models [86]:

- a) *animal models based on the induction of convulsions*: morphological abnormalities caused by convulsions induced by external epileptogenic effects can be studied.
- b) *genetic models*: gene modification is used to create specific animal strains to study the role of genetic factors in epilepsy.

In most preclinical studies of MTLE, rodents, either male rats or mice, are used, and two further study groups may be distinguished based on the number of seizures and the time course of the observation period:

- a) *acute models* (4 aminopyridine and febrile seizure model): Induce generalised epileptic seizures in healthy animals, causing single convulsions. They are created by artificial interventions, and the main drawback of this model is the lack of spontaneous recurrent seizure (SRS) activity.

- b) *chronic models* (models based on SE induction and kindling): These can be used to study epileptogenesis and interictal epileptogenic lesions. Spontaneous recurrent convulsions are also observed in experimental animals after a latent period [11].

1.9. Status epilepticus

Status epilepticus (SE) is a condition in which several seizures occur repeatedly and last at least half an hour. This is life-threatening for both patients and test animals as well. After altering blood pressure (first increasing and then falling), a state of metabolic acidosis develops (falling the partial pressure of oxygen in the blood and parallel to it rising the carbon dioxide, a fall in pH). The glucose level of the blood decreases and the ionic balance is altered, which eventually affects the kidneys. Heart failure causes pulmonary and brain oedema. This multiorgan failure eventually leads to death.

In SE animal models, the mortality is high enough, but in the majority of surviving animals, the morphological changes that are characteristic of MTLE and were listed in detail previously in 1.7 begin to develop. The most important is the neuronal loss in CA1, CA3, and subiculum areas, which resembles HS. Similar lesions have been observed in primate studies using mechanical ventilation, suggesting that the observed alterations are likely induced by electroconvulsions and not cardiorespiratory changes [86].

1.10. The murine model of pilocarpine-induced epilepsy

Pilocarpine-induced rodent epilepsy is one of the most widely used preclinical rodent models [5, 87] to study the underlying mechanisms of human MTLE.

In this model, following systemic pilocarpine administration, generalized motor convulsions develop that typically last for more than 1h. Most animals have SE with significant mortality, but the surviving animals enter a latent phase without apparent symptoms, showing recovery and normalisation of vital signs. However, after this latent phase, in the third, chronic phase, pilocarpine-treated (PILO) animals exhibit SRS [5, 87, 88]. SRS in rodents may be defined as involuntary motor episodes that can range from brief, nearly undetectable muscle twitches to long periods of vigorous shaking. During SE, mild to severe respiratory failure associated with cerebral hypoperfusion is observable. These abnormalities lead to hypoxia and hypoglycaemia, to which neurons are very sensitive. Brain damage is proportional to the length of SE and the frequency of SRS [5, 87, 89]. We must note that acute SE already damages the brain through astrocytic swelling, neuronal damage, cell death, microglial activation, and damage to the blood-brain barrier (BBB) after SE during the first week of survival [90-92]. These complex

neuropathological events initiate ongoing neuronal degeneration, which ultimately results in HS [93] months after pilocarpine injection [5, 87, 94].

Pilocarpine (Table 1) is a lipophilic BBB penetrating drug that acts as a cholinomimetic agonist of muscarinic acetylcholine receptors [5]. Pilocarpine triggers seizures originating from the limbic system through a double action. The convulsive effect is initiated directly by activating inhibitory muscarinic type 2 receptors (M2R) located in the presynaptic membrane of GABAergic inhibitory interneurons in the hippocampus, thus reducing GABA release [95]. Furthermore, pilocarpine can directly stimulate septal GABAergic neurons projecting onto hippocampal GABAergic interneurons through muscarinic type 3 receptors (M3R), causing disinhibition of excitatory neurons leading to the release of excess glutamate (GLU). This reduced inhibition of PCs and GCs creates a state of hypersensitivity and hyperactivity that is ultimately responsible for SE induction involving the hyperactivation of N - methyl - D - aspartic acid (NMDA) receptors [5, 23, 96].

In the pilocarpine model, the neuropathological lesions observed in the chronic period are similar to those of HS identified in human MTLE. Rodent epilepsy models exhibiting long-lasting SRS cause permanent brain damage, shown by shrinkage of the hippocampus and amygdala, similar to MTLE patients [97]. Histological analysis reveals that pilocarpine-induced SRS causes variable loss of PCs and MCs, strong sprouting of mossy fibres, and reorganisation of the ionotropic Glu receptor subunits in the hippocampus [5, 87, 89, 98, 99]. Parallel studies in patients and animal models indicate that the appearance of hypersynchronous neuronal discharges is responsible for the generation of spontaneous motor seizures [100]. Persistent hyperactivity of dentate interneurons and neuronal degeneration result in a loss of balance between the excitatory and inhibitory neuronal circuits in HF [100-102]. These convulsing animals are often used for pharmacological studies to develop antiepileptic therapeutic strategies [103-106].

From the point of view of late pathomorphology, the pilocarpine-induced epilepsy model and MTLE show the following similarities:

- Destruction of the PCs of CA1 and CA3 region, MCs, and hilar interneurons [107].
- Abnormal activation of GCs shown by increased expression of met-enkephalin /Met-Enk/ and neuropeptide-Y /NPY/ followed by mossy fibres sprouting over time [89, 108].
- In addition to astrogliosis, signs of angiogenesis are also observable [109].

All of these together eventually lead to scarring shrinkage of the hippocampus, which is termed HS in the literature [110].

Based on the results of animal models so far, there are three alternative theories for the pathomechanism of MTLE development:

1. Hypothesis of mossy fibre sprouting: Due to the destruction of hilar MCs and interneurons, mossy fibres grow abnormal collaterals toward adjacent GCs, and the resulting strong excitatory feedback causes hypersensitivity [79].
2. Dormant basket cell theory: Significant damage to hilar MCs results in loss of innervation of inhibitory interneurons, leading to reduced inhibition in GCs [111].
3. The death of inhibitory interneurons in the hippocampus is the main trigger of epileptogenesis [112].

1.11. Measure of spatial learning and memory

The complex neuropathological phenomena of HS coincide with significant cognitive disturbances in human patients [113]. Functional and morphological damage to the hippocampus in drug-induced preclinical rodent models can be assessed not only by neuropathological but also by behavioural studies, as the hippocampus is a key brain structure involved in memory formation and spatial navigation.

There are numerous behavioural tests to assess navigational learning and memory in rodents. By their nature, rodents are motivated to avoid open spaces and bright lights [114, 115]. The Barnes maze is based on this aversion that encourages them to search for shelter in the escape box (EB) and this test is best suited to the rodents' lifestyle. The Barnes maze is a dry-land-based rodent behavioural paradigm to assess spatial learning and memory, which was originally developed by its namesake, Carol Barnes [116]. The basic function of the Barnes maze is to measure the ability of a mouse to learn and remember the location of a target zone using a configuration of distal visual cues located around the testing area [117]. This non-invasive task is useful for identifying cognitive deficits in neurological diseases, such as epilepsy. Various parameters are measured including latency to escape, path length, velocity, and number of errors. We also preferred the Barnes maze to the Morris water maze (another popular maze), because it does not involve swimming, which can be perceived as stressful and increases corticosterone levels. Furthermore, swimming also causes a reduction in core body temperature, which can affect performance.

Recently, a new, sensitive scoring system has been developed for mouse EB search strategies for both initial training and for changing the escape target to a new position. These strategy scores add an important dimension to the time and path length data that help to evaluate the results in this popular maze [118].

1.12. Potential neuroprotective effect of kynurenic acid and its synthetic analogue SZR104 in preclinical epilepsy models

Generalised motor convulsions cause neuronal damage, astrocytic swelling, and the opening of the BBB [103, 119, 120]. These primary neuropathological findings will initiate subsequent neuroinflammatory cascades. The opening of the BBB gives way to blood-borne immune cells that enter the brain parenchyma [121, 122]. Local microglia activation releases cytokines that further stimulate neuroinflammation (e.g., microvessel sprouting and macrophage migration). Endogenous kynurenic acid (KYNA, also known as 4-hydroxyquinolin-2-carboxylic acid with the chemical formula $C_{10}H_7NO_3$) (Table 1) plays a key role in various neuroinflammatory and neurodegenerative disorders of the CNS [123, 124]. KYNA has been shown to have anti-inflammatory effects on the CNS, which can contribute to its neuroprotective actions.

By modulating glutamatergic neurotransmission through its antagonistic effects on the NMDA receptor, KYNA can help regulate neuronal excitability and protect against excitotoxicity, in which excessive activation of Glu receptors leads to neuronal damage [123, 124].

Exogenous KYNA can not penetrate the BBB effectively, limiting its potential therapeutic applications [125]. By synthesising KYNA analogues, particularly SZR104 (N-(2-(dimethylamino) ethyl)-3-(morpholinomethyl)-4-hydroxyquinoline 2-carboxamide, with chemical formula $C_{19}H_{26}N_4O_3$) (Table 1) that can traverse the BBB and reach the brain, the researchers hope to unlock new treatment possibilities for neurodegenerative disorders characterised by neuroinflammation and neurodegeneration [126]. In a study involving rats under urethane anaesthesia, SZR104 was investigated for its effects on pentylenetetrazol (PTZ) seizures, a commonly used model to study seizure activity. The results of the experiment indicated that pretreatment with SZR104 significantly decreased the seizure-evoked field potentials in PTZ-induced convulsions. This suggests that SZR104 may have anticonvulsant properties and could potentially be beneficial in the treatment of seizures [126].

Using a mouse model of pilocarpine-induced generalised epilepsy is a common approach in epilepsy research, as it can mimic certain aspects of human epilepsy. The fact that acute generalised convulsive seizures increase the extracellular concentration of Glu in the brain is an important finding that suggests a possible mechanism underlying epileptic activity [127].

KYNA affects the immune system in the brain, particularly through the regulation and modulation of effector immune cells [128], such as microglial cells. These cells play a crucial role in the immune response of the brain and are known to be involved in the progression of various neurological disorders, including epilepsy [129-131]. Microglial cells can be activated

and transformed by a variety of signals, including neurotransmitters such as Glu, damage-associated stress signals, cytokines, colony-stimulating factors, and free radicals [132-134].

When activated in response to disease or injury, microglia can adopt a phenotype known as reactive microglia (=disease-associated microglia, DAM), which undergo significant morphological changes, such as increased area and development of more cytoplasmic processes [129, 130, 132]. Although DAM can play a protective role in clearing debris and pathogens, they can also contribute to neuronal damage and cell death. This complex interaction between microglia and neurons underscores their crucial role in maintaining brain homeostasis and responding to various pathological conditions.

Understanding the specific pathways through which SZR104 operates and its interactions with the neural and immune systems may provide important information to optimise its therapeutic potential. Our interest focused on the potential anticonvulsant effect of SZR104, thus, we tested it in NMRI strain mice as a potential drug candidate. Through observation of the proliferation tendency and area of hippocampal microglial cells, researchers can gain insight into how these immune cells respond to epileptic activity and whether interventions such as SZR104 can modulate their functions. A proven method to study hippocampal microglial cells by immunohistochemistry of ionised calcium-binding adaptor molecule 1 (Iba1) [135].

In addition to the microglial cell assays mentioned above, in the same study, we found inhibition of microglial phagocytosis and a decrease in blood levels of interleukin-6 (IL-6) after SZR104 administration, suggesting a possible anti-inflammatory effect of this compound [136].

2. Aims

The specific aims of the present studies were the following:

- 1) We set out to characterise in detail the neuropathology of HS that develops over the course of 3.5 months of pilocarpine-induced SRS in NMRI mice, as such data in the literature were sparse/lacking despite the fact that the NMRI mouse is a widely used strain in epilepsy research.
- 2) We were especially interested in studying PARV-immunopositive, and CALR-immunopositive interneurons in our HS model, as the integrity of these interneurons is crucial not only for normal hippocampal functions but also for seizure-induced pathological alterations.
- 3) We also aimed to study the effects of pilocarpine-induced SRS on spatial learning and memory processes in the NMRI mouse strain.
- 4) We investigated the acute pharmacological effects of the synthetic KYNA analogue SZR104 on seizure-induction and microglial activation 24 h after in our murine pilocarpine-induced epilepsy model.

3. Materials and Methods

3.1. Experimental protocol and pharmacological treatment

All behavioural experiments were performed in the light period. In these studies, adult, male, six-week-old NMRI strain mice were used. (body weight [bwt] = 28 - 36g). We chose this strain, because the MCs of NMRI mice were found to be highly susceptible to pilocarpine treatment according to the literature [94]. The animals were housed under standard environmental conditions (temperature controlled room (24°C±1°C, humidity 22%±2%) under standard dark/light cycle (12 - 12 h). Standard mouse chow and tap water were supplied *ad libitum*. All experimental procedures, handling, and housing of the animals were carried out in accordance with the European Union Directive ('Directive 2010/63/EU of the European Parliament and of the Council of 22 September 2010 on the Protection of Animals Used for Scientific Purposes') and according to the Hungarian Animal Act. Specific approval for the care and use of animals was obtained in advance from the Faculty Ethical Committee on Animal Experiments (University of Szeged; 1-74-1/2017. MÁB) and from the Government Office (Department of Food and Animal Health) of Csongrád County (CS/101/3347-2/2018).

The experimental animals in the first study (n = 50), who underwent memory and learning tests, were divided into two experimental groups: pilocarpine-treated (PILO, n = 40; for the structure of pilocarpine, see Table 1) and controls (n = 10). During the experiment and after the treatments, the animals were individually labelled on the tail skin and observed daily in their cages to note the SRS of the PILO mice. The daily observation time was 1 h in a 9 - 10 a.m. period. The observation period lasted 3.5 months after pilocarpine treatment.

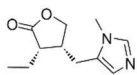
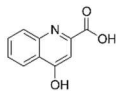
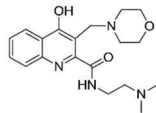
Code	Molecular Structure	Chemical Name	Empirical Formula
Pilocarpine		3-ethyl-4-[(3-methylimidazol-4-yl)methyl]oxolan-2-one	C ₁₁ H ₁₆ N ₂ O ₂
KYNA		4-hydroxyquinolin-2-carboxylic acid	C ₁₀ H ₇ NO ₃
SZR104		N-(2-(dimethylamino)ethyl)-3-(morpholinomethyl)-4-hydroxyquinoline-2-carboxamide	C ₁₉ H ₂₆ N ₄ O ₃

Table 1. Molecular structure, chemical name, and empirical formula of pilocarpine, KYNA, and SZR104.

PILO animals received a single dose of pilocarpine (Sigma-Aldrich Co., St. Louis, MO, USA) dissolved in sterile physiological saline (provided by the Central Pharmacy Laboratory of Albert Szent-Györgyi Medical School, University of Szeged, Hungary) and injected intraperitoneally (i.p.). 195 mg / kg of pilocarpine were found to be appropriate for NMRI mice to precipitate motor seizures [94]. 90 min after the first motor symptoms of epileptic seizures, 10 mg/kg diazepam was injected i.p. (Seduxen®, Gedeon Richter Plc, Budapest, Hungary) to terminate motor convulsions. Post-seizure treatment included continuous observation and intradermal and i.p. injections of Krebs-Ringer bicarbonate buffer solution (bicarbonate buffered isotonic saline containing magnesium, potassium, sodium, and glucose; Merck KGaA, Germany) during the first 24 h.

Approximately half of the animals displaying seizures died on the day of the pilocarpine treatment. Nine animals survived for 3.5 months and one animal perished at 3 months; therefore, it was not used for spatial learning tests, obviously. This mouse (PILO10) will be shown as a case report after our results. Therefore, the overall mortality of pilocarpine-induced epilepsy in this study slightly exceeded 75% at the 3.5 months timepoint.

The control animals were injected i.p. with the same volume of physiological saline, the solvent of pilocarpine. These animals displayed normal behaviour and did not receive injections of diazepam or Krebs-Ringer solution.

After the survival period, PILO animals (n = 9) together with controls (n = 9) were used in the Barnes maze test, then the animals were sacrificed and their brains were investigated with immunohistochemical techniques (Table 3).

In the second study, we tested the effects of SZR104 (for the structure of SZR104 see, Table 1) pretreatment in pilocarpine-induced epilepsy. In this study, epilepsy was induced in the aforementioned way. The animals were divided into four groups (n = 10/groups; see Table 2). Control animals received physiological saline i.p., SZR104 was dissolved in distilled water and administered i.p. at a dose of 358 mg / kg 40 min before pilocarpine injection according to [126]. On day of treatment, mortality was similar to the case of the first study of animals displaying convulsions, approximately 50% of PILO mice and animals injected with SZR104 + pilocarpine. Post-seizure treatment was the same as mentioned above.

One day (24 h) after treatment, the surviving animals were sacrificed and the brain and blood were further processed [90]. Four animals of each group were investigated with immunohistochemical techniques.

Pharmacological treatment	Number of surviving animals	Experimental procedures
Control 0.9% NaCl i.p. injection	10	Blood samples (6 animals). Immunohistochemistry (4 animals)
PILO 195 mg/kg pilocarpine i.p. injection	10	Blood samples (6 animals) Immunohistochemistry (4 animals)
SZR104-treated (358 mg/kg) i.p. injection	10	Blood samples (6 animals) Immunohistochemistry (4 animals)
SZR104-treated (358 mg/kg) + PILO (195 mg/kg pilocarpine) i.p. injections	10	Blood samples (6 animals) Immunohistochemistry (4 animals)

Table 2. Animals used in the second study (SZR104 pretreatment) for pharmacological-immunohistochemical experiments and blood sampling.

3.2. Tissue preparation

In the first study 3.5 months after pilocarpine injections (and two weeks after the Barnes maze test), as well as one day after in the second study (SZR104 pretreatment), the animals were sacrificed:

Mice were deeply anaesthetised with halothane (Sigma - Aldrich, St. Louis, MO, USA) and transcardially perfused with 30 mL of physiological saline followed by 30 mL of cold 4% paraformaldehyde in 0.1 M phosphate buffer (PB; pH 7.4). The brains were removed and post-fixed in the same solution for 5 h, then cryoprotected overnight in 30% sucrose in 0.1 M phosphate buffer (PB, pH 7.4) at 4 °C. Coronal brain tissue blocks were cut using an acrylic brain slicer matrix (Zivic Instruments, Pittsburgh, PA, USA). Coronal plane sections were cut to 24 µm thickness from the hippocampus between the coronal levels Bregma - 1.06 mm and Bregma - 2.30 mm [137] according to the Allen's Mouse Brain Atlas (www.brainmap.org) on a freezing microtome (Reichert-Jung, Cryocut 1800) and the sections were stored at 4 °C in a PB solution containing 0.1% NaN₃ until further processing.

3.3. Immunohistochemistry

Free-floating sections were used for immunohistochemistry (IHC). Endogenous peroxidase activity was blocked with 3% H₂O₂ for 15 min. Nonspecific binding sites were blocked with 20% normal pig serum (NPS; diluted: 1/10) and tissue permeability was enhanced by using 1% Triton X-100 in blocking NPS solution. Sections were incubated overnight at room temperature (RT) in primary antibody solutions with the following primary antibodies (Table 3):

rabbit anti - neuropeptide-Y (NPY; 1/10000, Abcam, Cambridge, UK); mouse anti-Neuronal N (NeuN; 1/8000, Chemicon, Temecula, CA, USA); rabbit anti-Iba1 (Iba; 1/8000, FUJIFILM Wako Chemicals Europe GmbH, Germany), goat anti-calretinin (CALR; 1/20000, Millipore, Temecula, CA, USA), mouse anti-parvalbumin (PARV; 1/40000, Sigma-Aldrich, St.Louis, MO, USA). Biotinylated secondary antibodies (1:400 dilution, Jackson Immuno Research, West Grove, PA, USA) were used for 1 h at RT and the signal was detected with peroxidase-labelled streptavidin (1/6000, Rockland Immunochemicals Incorporation, Limerick, PA, USA) for 1 h at RT. All incubations were performed in plastic vials with continuous agitation. Immune reaction sites were visualized with diaminobenzidine tetrahydrochloride (DAB)+H₂O₂ in the absence (30 min reaction time) or presence (15 min reaction time) of 0.3% nickel sulphate (used only with the NPY antibody). Sections were mounted on microscope slides, air-dried, dehydrated, and cover-slipped with dibutyl phthalate xylene (Merck KGaA, Germany). Chemicals other than antibodies were purchased from Sigma-Aldrich (Sigma-Aldrich, St. Louis, MO, USA).

	Primary antibody	Secondary antibody	Tertiary reagent	Visualization
1	m NeuN	B-GAM	STA-PER	DAB
2	r NPY	B-GAR	STA-PER	DAB + Ni
3	r Iba1	B-GAR	STA-PER	DAB
4	g CALR	B-DAG	STA-PER	DAB
5	m PARV	B-GAM	STA-PER	DAB

Table 3. Reagents used for IHC.

3.4. Spatial learning test using the Barnes maze

Three months after injections, the experimental animals (control n = 9, PILO n = 9) were tested for 4 consecutive days in a hippocampus-related learning paradigm, Barnes maze, to measure spatial learning and memory capabilities [138]. Handling was carried out daily, at the same time, and started one week before the experiments. The animals were kept in isolation at all times and were always cared for and tested by the same investigators to ensure that nothing affected the results.

The experiments were carried out in a well-lit testing room with a holding room located in the vicinity. The Barnes maze apparatus (Figure 2) consists of an elevated circular black surface arena (plate diameter: 100 cm, thickness 1 cm, the plate is located 90 cm above the floor) with 18 circular holes around its circumference. Almost all holes lead to an open drop to the floor, only one of them allows escape and contains EB underneath, where the animal can hide [139]. The small experimental room is equipped with relatively large visual cues, such as coloured

shapes attached to the wall to allow the mice to learn the location of the holes. The surface of the arena is lit brightly with an overhead light source. The EB can be reached through the corresponding hole on the tabletop. We did not change the location of the EB during the whole experiment. The animals were placed in a non-transparent starting cylinder in the centre of the arena for 10 sec. After lifting the cylinder, the mice were given a maximum of 5 min to explore the maze and finally allowed to be in the EB for 15 sec. When a mouse did not find the target, it was gently guided by hand or placed in the hole and allowed to spend the same amount of time in the box. The time needed was measured with a chronometer by the investigators. All animals performed two trials per day with a constant inter-trial interval of 4 hours, for three days. After a few trials, rodents typically remember which hole contains the drop box on its own and quickly proceed in a direct path toward the hole. On the probe day there was only one trial in the morning (4th day is equal to the probe day). The plate and the EB were cleaned with 70% ethanol after each session and each animal, in order to eliminate olfactory cues. No video tracking was used, the performance was evaluated through the measurement of the total latency, which means the time needed to find the EB with the whole body from when the animal was released from the start box. The daily latency measurements were statistically analysed. We compared the mean daily latencies in controls and in PILO animals [140]. Measurements were also analysed in relation to time: daily latencies were plotted as Y values (dependent variables), while days were plotted as X values (independent variables).

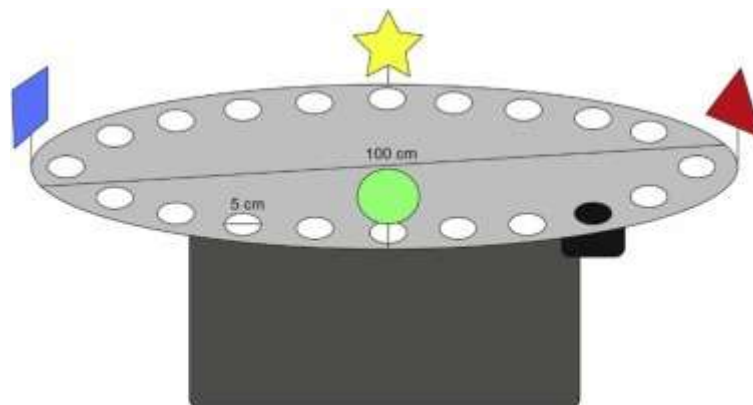


Figure 2. Schematic drawing of the Barnes maze arena [118].

3.5. Morphometry and evaluation of data

The immunostained sections were scanned with a Slide scanner (Mirax Midi, 3DHistech Ltd., Budapest, Hungary) equipped with a Panoramic Viewer 1.15.4, CaseViewer 2.1 programme and a QuantCenter, HistoQuant module (3DHISTECH Ltd., Budapest, Hungary). Using the digital image, the area of interest (AOI) was manually outlined.

Immunostainings were quantified with the DensitoQuant application of the QuantCenter (3DHISTECH Ltd., Budapest, Hungary). The application identifies the positive stain, based on the automatic colour separation method, through which individual positive pixels are counted and classified according to intensity and threshold ranges. In this way, the software calculates a staining density score based on the proportion of positive and negative pixels. In the case of NeuN and Iba1 stainings, density score measurements from each animal (control $n = 9$, PILO $n = 9$) were used (4 sections and 8 hippocampi per animal). The measured density values were averaged per animal and used for statistical processing.

The area of HF was also examined by the QuantCenter in sections stained by NeuN (control $n = 9$, PILO $n = 9$). The mathematical mean of the data was statistically evaluated to illustrate the shrinkage of HF in PILO animals.

PARV- and CALR-immunostained cells were also counted by the QuantCenter, using the digitised images. Cells that had sharp contours and processes were counted only and then the number of these cells was corrected to a 1mm^2 area of the HF.

For the evaluation of IHC results and the behavioural test, a Student's t-test for independent samples was used. The results of the statistical analyses were reported according to Khakshooy and Chiapelli [140].

For statistical analysis, SPSS software (IBM SPSS Statistics 24) was used and the results were expressed as mean \pm (SEM). Statistical significance was generally set at $p < 0.05$.

In the second study, the digitised sections were analysed using Image Pro Plus 4.5 morphometry software (Media Cybernetics, Silver Spring, MD, USA). Four sections from each animal were analysed. The threshold was determined in such a way that the counting programme could equally recognise immunoreactive microglial cells of Iba1. The software counted the number of immunostained cells in the entire AOI. The number of microglial cells in the AOI has been normalised to 1mm^2 . The surface area of the single microglial cells was also measured with the help of Image Pro Plus 4.5 software. Single microglial cells were selected from digital images with 3000x magnification, their contours were manually outlined, and their area was measured. Selection and measurements were relatively simple due to the low staining background and the strong Iba1 immunostaining of the microglial cells. Ten microglial cells were selected from the hippocampi of each experimental group. These cell area measurements were expressed as μm^2 values. Data are expressed as mean \pm SEM, differences were calculated with ANOVA, Bonferroni post hoc test ($p < 0.05$ was significant). GraphPad Prism8 software (version 8.4.3) (GraphPad Software, LLC, San Diego, CA, USA) was used to statistically analyse the results of the immunohistochemical measurements.

4. Results

4.1. Neuronal loss and shrinkage of the hippocampus 3.5 months after SE

We measured the optical density of the NeuN immunostaining: the area of interest (AOI) was the entire HF. The subiculum contained neurons in every PILO animal, although we did not separately assess the density in this sector. NeuN-stained cells disappeared mainly from the *stratum pyramidale* of the CA1, CA2, and CA3 sectors in PILO1, 3, 4, 7, 8, 9 animals (Table 4; Fig. 5C). In these animals, scattered NeuN-stained cells were present only in *stratum oriens*, *radiatum*, and *lacunosum-moleculare* (Fig. 5C). These cells were probably interneurons. In animal PILO2, the *stratum pyramidale* appeared to be intact in CA1, but these principal neurons of CA2 were completely degenerated. In PILO8, the *stratum pyramidale* in CA1 and CA3 showed patchy neuronal loss: neurons were missing in 100-200 μm long periods. GCs of DG did not show a spectacular loss, although in PILO6-7 mice, the lateral tip of the layer of the upper blade of *stratum granulosum* was thinner than in normal. Small NeuN-stained cells were scattered, suggesting a decrease in the number of GCs in this area. On the other hand, thickening of the rest of the *stratum granulosum* in DG was observed in animals with HS, suggesting dispersion of GCs, but they were not counted separately [93, 104]. The location of neuronal degeneration in individual PILO animals is summarised in Table 4.

PILO animals	Location of neuronal loss in HF stained with anti-NeuN serum in light microscopic images
PILO1	CA1, CA2, CA3 are degenerated
PILO2	only CA2 is degenerated
PILO3	CA1, CA2, CA3, and hilum are degenerated, GCs are dispersed
PILO4	CA1, CA2 and CA3 are completely degenerated
PILO5	cell loss in CA1, CA3, and hilum
PILO6	cell loss in hilum and upper blade of the GCs of DG
PILO7	CA1, CA2, and CA3 are completely degenerated, and minor loss of the upper blade of the GC layer of DG was present
PILO8	patchy neuronal loss is in <i>stratum pyramidale</i> of CA1 and CA3
PILO9	CA1, CA3 are degenerated, partial loss in hilum, CA2 is normal

Table 4. The degree of HS and the location of neuronal degeneration in PILO mice. The fields of CA, the hilum, and the *stratum granulosum* of DG are indicated. Observations are based on qualitative light microscopy of NeuN-immunostained histological sections of HF.

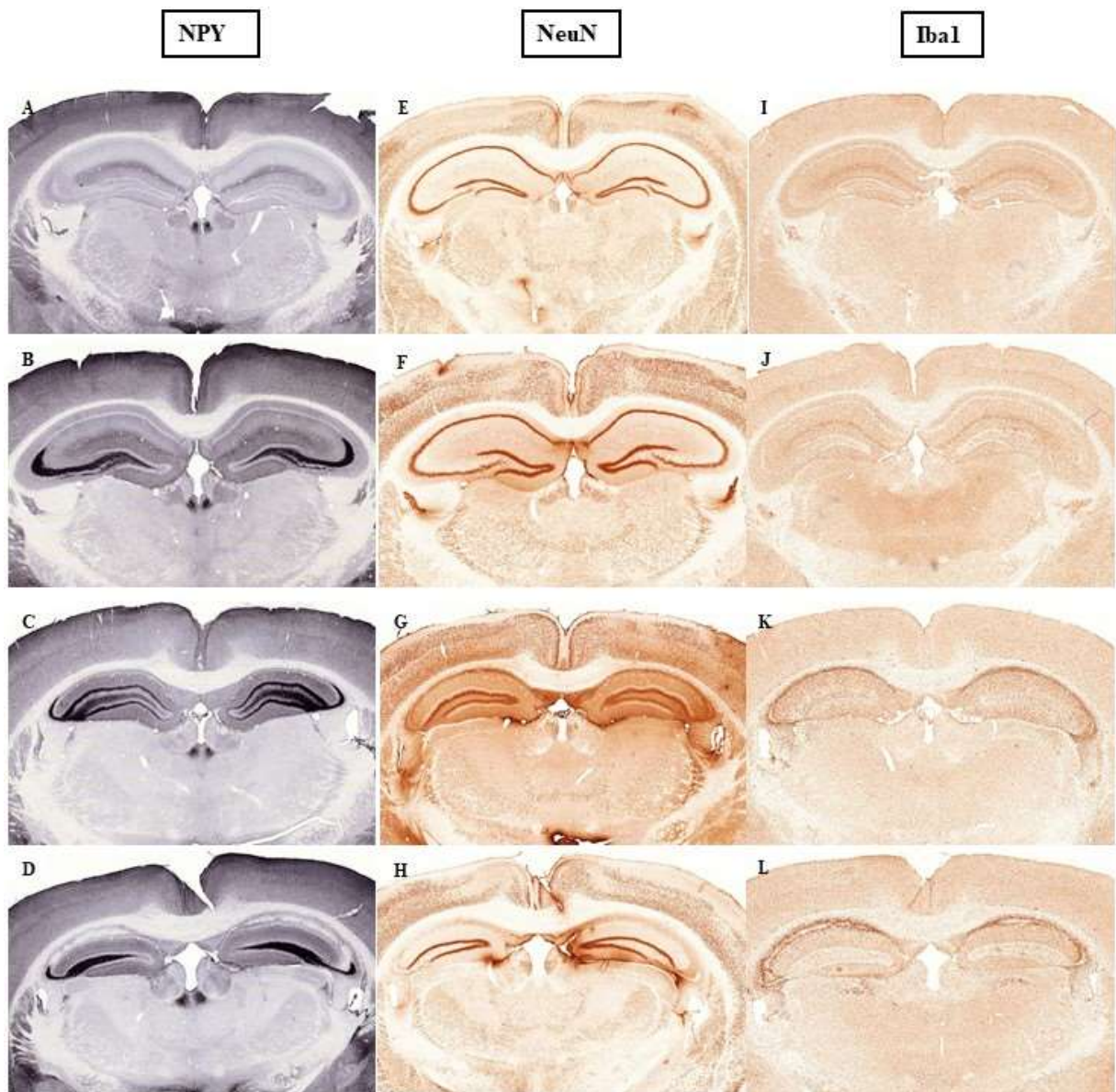


Figure 3. Representative images of NPY, NeuN, and Iba1 immunostainings in the mouse hippocampus: Control animals (A, E, I); PILO animals (B-D, F-H, J-L); PILO animals exhibiting sclerotic hippocampi (C-D, G-H, K-L).

Observation of PILO mice proved the development of regularly repeated behavioural seizures, and the resulting gradual degeneration of the hippocampus is visible in the IR images with NeuN, NPY and Iba1 stainings (Fig. 3).

We detected neuronal loss with NeuN-labelling (Fig. 3F-H), microglial proliferation with Iba1-labelling (Fig. 3J-L), and axonal sprouting with NPY immunostaining (Fig. 3B-D) [93].

Neuronal loss and microglial proliferation overlapped in all cases, indicating the presence of ongoing neuronal degeneration in the hippocampus (Fig. 3F-H, J-L).

All animals with behavioural seizures showed greatly enhanced NPY immunoreactivity in the DG (Fig. 3B-D). PILO mice showed various degrees of hippocampal degeneration and thinning of the fimbria, and five of the PILO animals showed HS, two of them are shown in Fig. 3C-D. Another standard sign of HS was the increase in the density and thickness of the NPY immunoreactive band in the inner molecular layer of DG and CA3, attributed to the sprouting of the mossy fibres of GCs.

Marked neuropathological changes were found in animals with HS:

- 1) PCs and MCs disappeared completely, as revealed by immunohistochemistry for NeuN (Fig. 3H). The less serious stages of hippocampal degeneration showed segmental loss of PCs in CA1 and CA3 (Fig. 3G).
- 2) The density of immunoreactivity for the microglial marker (Iba1) increased significantly (Fig. 3K-L). The morphological properties of the microglial cells changed dramatically in the affected areas (Fig. 3C-E).

Densitometric analysis of NeuN staining in the hippocampus (subiculum, CA1, CA2, CA3; Fig. 4A) and in the DG (hilum, *stratum granulosum* and *moleculare* (Fig. 4B)) proved a significant loss of neurons in PILO animals (Fig. 4A,B). Statistical analysis of the NeuN-staining densities showed an approximately 50% loss of immunostaining in the CA regions, and an approximately 30% loss in the DG (Fig. 4A,B).

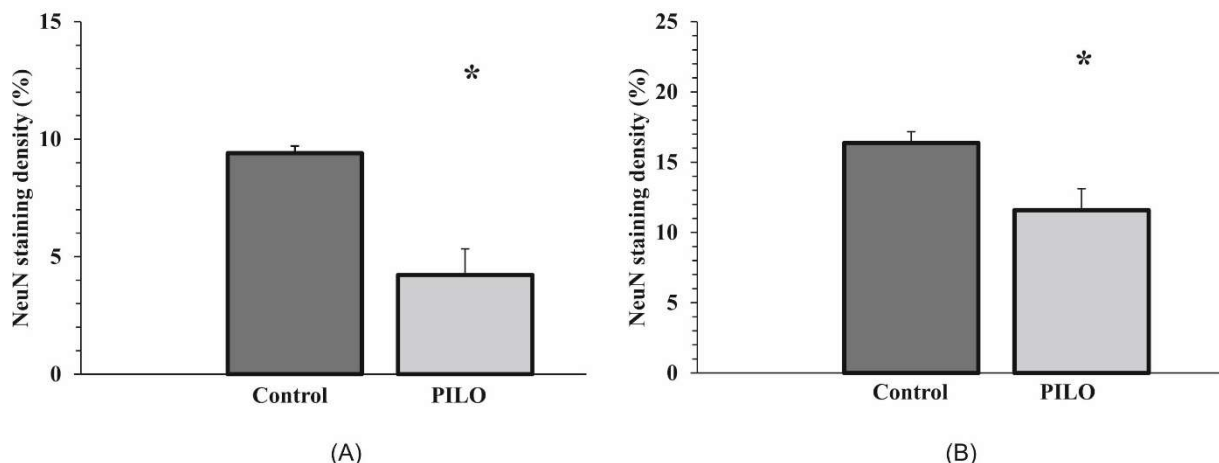


Figure 4. Densitometric analysis of NeuN-stained hippocampi: NeuN staining density throughout the CA region in control and PILO animals (n = 9/groups; paired t-test, * $p = 0.001$) (A). NeuN staining density in the entire area of the DG in control and PILO animals (n = 9/groups; paired t-test, * $p = 0.016$) (B).

Qualitative analysis of the NeuN-immunostained sections proved that every PILO animal displayed some degree of HS (Fig. 6C). According to the significant neuronal loss, the measured sectional area and the diameter of HF decreased significantly in epileptic mice, indicating shrinkage of HF (Fig. 5A,B).

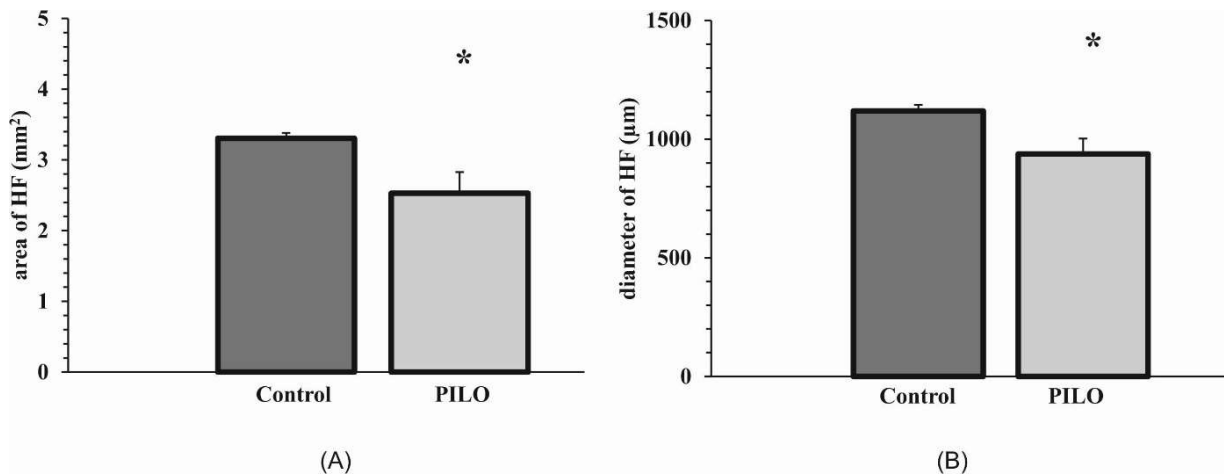


Figure 5. Decrease in cross-sectional area (A) and diameter (B) of HF in PILO animals compared to controls, measured in coronal sections in NeuN IHC (n = 9/groups; paired t-test, * $p = 0.043$ and 0.028 , respectively).

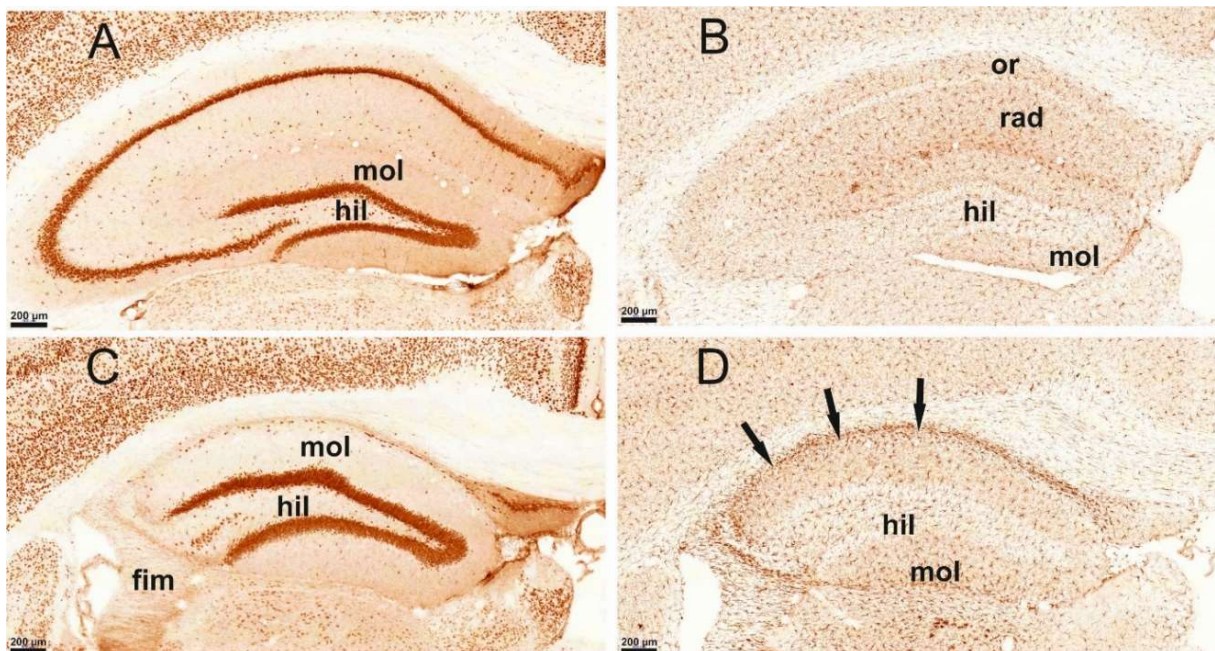


Figure 6. Representative photomicrographs of neurons (A, C) and microglial cells (B, D) in the control (A, B) and PILO4 (C, D) hippocampi. NeuN immunostaining (A, C) revealed a complete loss of principal neurons in the CA regions of PILO4 (C). Iba1 staining revealed an accumulation of microglial cells in the sclerotised regions, as indicated by the arrows (D). Abbreviations: **mol** = *stratum moleculare* of DG; **hil** = hilum of DG; **or** = *stratum oriens*; **rad** = *stratum radiatum*; **fim** = fimbria. Scale bars: 200 µm.

4.2. Microglial activation and proliferation 3.5 months after SE in HF

Iba1 - IR microglial cells were found scattered in control HF (Fig. 6B). Cell bodies were small, processes were slender and relatively short, like in the second study (Fig. 15A). Epileptic HF contained significantly higher numbers of Iba1-immunostained microglial cells (Fig. 6D). The significant increase in the density of Iba1 staining is shown in Fig. 7. These DAM cells were larger, the processes were thicker, longer and more numerous than those of the controls, similar to the case of the second study, representative images are shown there (Fig. 15B,C). Comparison of the hippocampus stained with NeuN and those stained with Iba1 resulted in a negative 'match': those hippocampal areas that lost their neurons contained a high number of enlarged microglial cells in, or close to the *stratum pyramidale* (Fig. 3F-H, J-L, Fig. 5C,D). The overall staining density of the microglia increased significantly in the HF of the PILO mice according to the increased number of microglial cells (Fig. 7).

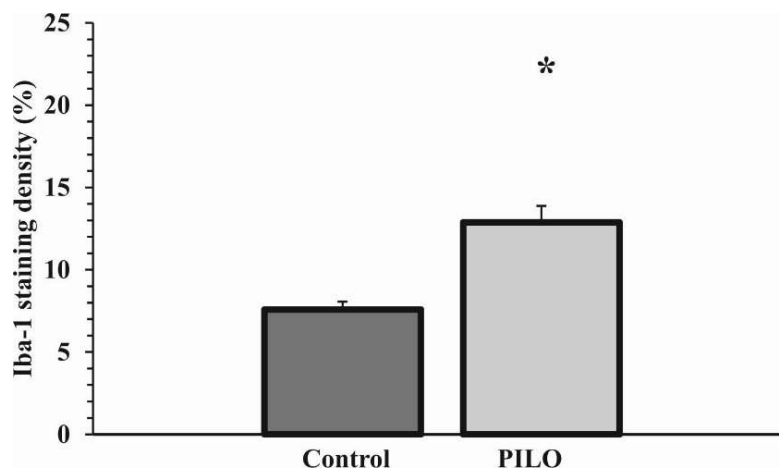


Figure 7. Increase in the density of Iba1 staining in HF in PILO animals compared to the controls (n = 9/groups; paired t-test, * $p = 0.012$).

4.3. Sprouting of mossy fibres 3.5 months after SE

Control mice displayed scattered NPY-immunopositive neuronal cell bodies in the hippocampus in the *stratum oriens*, *pyramidale*, and *radiatum*. DG has NPY-positive cell bodies in the hilum and close to the *stratum granulosum*, with processes sometimes extending between the GCs to the *stratum moleculare* (Fig. 3A, Fig. 8A). In this study, NPY-immunostained sections were qualitatively analysed. The dendritic processes of the cells also contained NPY immunoreactivity, mostly in the *stratum oriens* and *lacunosum-moleculare* of the CA3 sector, between the GCs and moderately in the *stratum moleculare* of DG (Fig. 8A). Axonal staining was not visible in controls (Fig. 8A). PILO mice presented strong NPY staining

of the neuropil throughout the hilum and in the *stratum lucidum* and *stratum oriens* of CA3 (Fig. 8B). Strong NPY-like staining presented in the inner molecular layer (IML) of the DG: these NPY immunoreactive (NPY-IR) elements are probably contacting the primary dendrites of the GCs (Fig. 8C). The location of NPY staining is very similar to Timm's reactivity of these areas described in the literature [94, 98]. Therefore, we believe that these elements are the sprouting axons [94, 98]. NPY staining of these hilar and CA3 areas was found in all PILO animals (Fig. 3B-D), regardless of the severity of neuronal cell loss. Even if there were no remaining nerve cells in CA3, the NPY-immunostained network was present in the area corresponding to the *stratum lucidum* of CA3 (Fig. 8C). Axonal sprouting was not quantified because it appeared as an all-or-nothing phenomenon, with no discernible NPY immunostaining in controls and strong NPY immunostaining in all PILO animal.

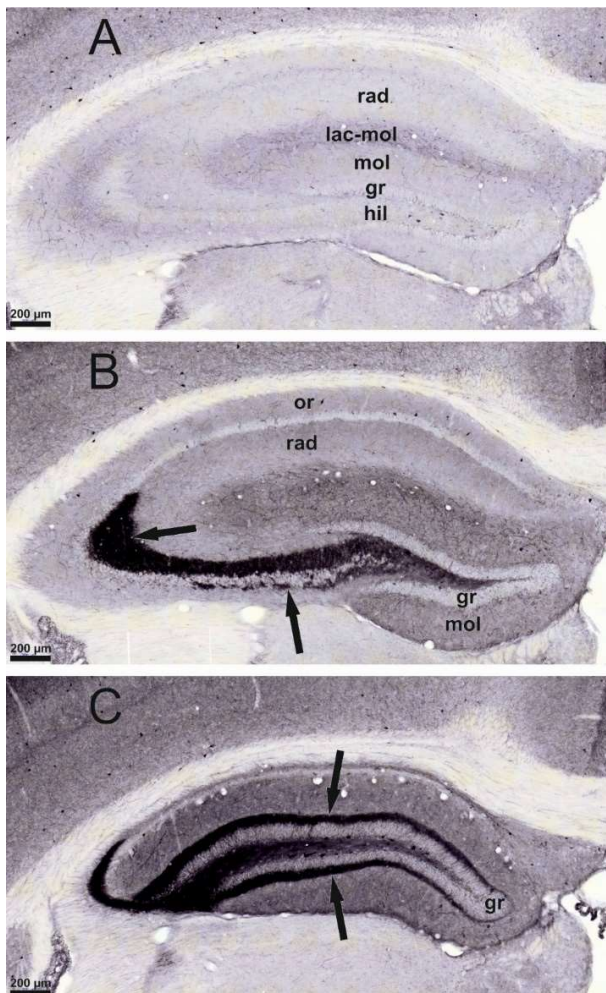


Figure 8. NPY immunostaining of control (A) and epileptic (B, C) hippocampi: PILO5 animal (B), PILO3 animal (C). Black staining indicates the NPY-containing sprouting axons in the hilum, in the *stratum lucidum*, and in the *stratum oriens* of CA3 (B, arrows). The IML of the DG is also heavily infiltrated by sprouting axons (C, arrows). Abbreviations: **rad** = *stratum radiatum*; **lac-mol** = *stratum lacunosum-moleculare*; **mol** = *stratum moleculare* of DG; **gr** = *stratum granulosum* of DG; **hil** = hilum of DG. Scale bars: 200 μ m.

4.4. Parvalbumin-containing hippocampal interneurons 3.5 months after SE

PARV-containing neurons were scattered in the HF: most of them were located in the *stratum pyramidale*, where a dense PARV immunoreactive (PARV-IR) fibre network was seen

(Fig. 9A). Scattered PARV-IR neurons were presented in the *stratum oriens* and *radiatum* (Fig. 9A). In the DG, PARV-IR cells were located in the *stratum granulosum* and hilum (Fig. 9A). Due to the different degrees of neuronal damage, we did not evaluate the regions of HF separately: in HS it was not possible to precisely determine the location of the CA sectors, so the total number of PARV-IR cells in the entire area of HF was counted. A significant decrease in the number of PARV-IR cells was found: some of the remaining PARV-IR cells were found in the hilum, in the *stratum granulosum* of DG, in the *stratum oriens* and *stratum radiatum* of CA, and some in the subiculum (Fig. 9B,C). These remaining PARV-IR cells showed strong immunoreactivity (Fig. 10A). We detected PARV-stained astrocyte-like cells in the *stratum lucidum* of CA3 and in the *stratum moleculare* and hilum of DG in the sclerosed hippocampi (Fig. 10B). The statistical data showed an approximately 50% decrease in the number of PARV-IR neurons in the HF of PILO animals compared to controls (Fig. 11A).

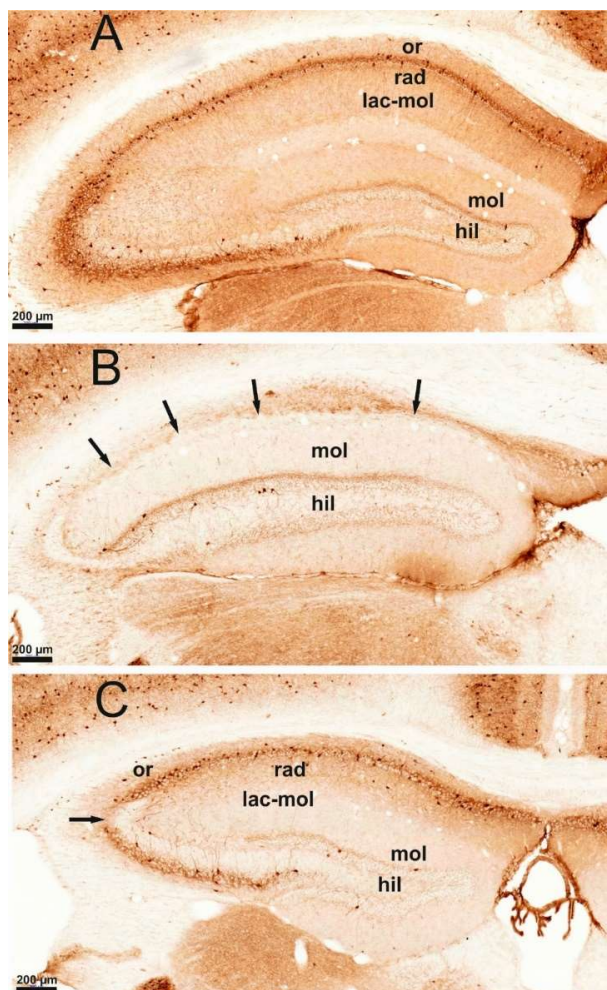


Figure 9. PARV staining of control (A) and epileptic (B, C) hippocampi. Note the scattered PARV-stained neurons and the pericellular PARV-stained axonal network in the layers of the principal neurons in the Control1 animal (A). In PILO7, there were no principal neurons in CA1-3, and the PARV-containing neurons also disappeared (arrows point at the location of the *stratum pyramidale*, without cells) (B). Patchy neuronal loss was detected in CA3 (arrow) of PILO8 animal (C). Abbreviations: **or** = *stratum oriens*; **rad** = *stratum radiatum*; **lac-mol** = *stratum lacunosum-moleculare*; **mol** = *stratum moleculare* of DG; **gr** = *stratum granulosum* of DG; **hil** = hilum of DG. Scale bars: 200 µm.

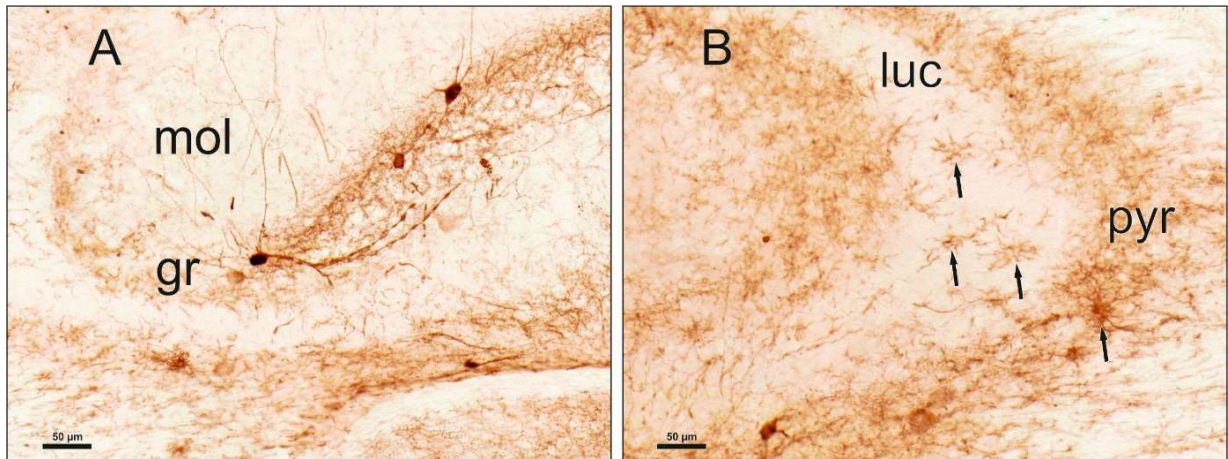


Figure 10. PARV-stained structures in PILO4 (A) and PILO7 (B) animals, with PARV-stained neurons between the neurons of DG in *stratum granulosum* (A). A fine pericellular PARV network is visible. PARV-stained astrocyte-like cells (black arrows) are visible in the *stratum lucidum* and *stratum pyramidale* of CA3 in PILO7. Abbreviations: **mol** = *stratum moleculare* of DG; **gr** = *stratum granulosum* of DG; **pyr** = *stratum pyramidale* of CA3; **luc** = *stratum lucidum* of CA3. Scale bars: 50 μm .

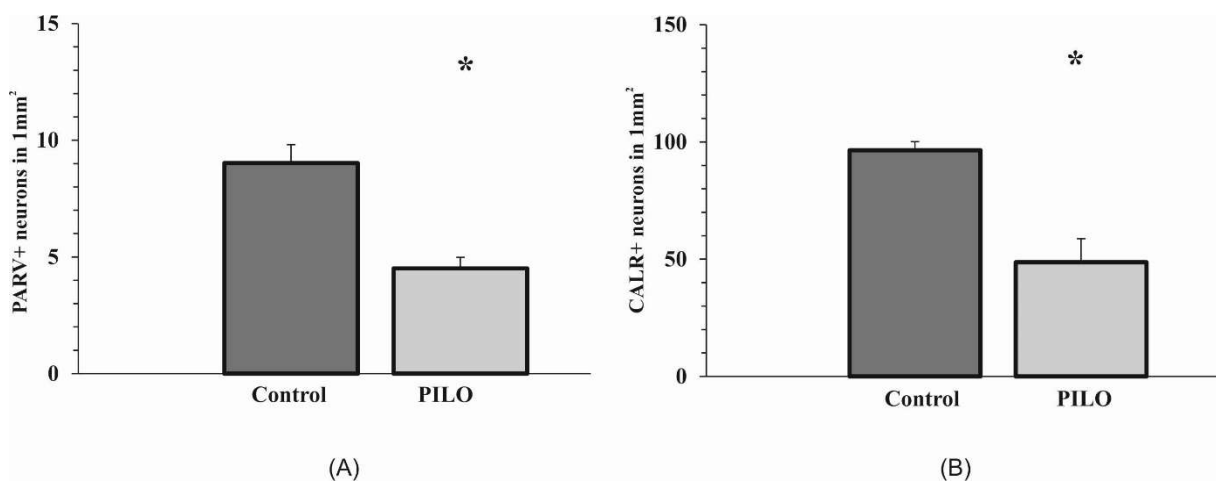


Figure 11. The number of PARV-containing neurons in the HF in control, and PILO animals (paired t-test, $*p < 0.0001$) (A). The number of CALR-containing neurons in HF in control, and PILO animals (paired t-test, $*p < 0.001$) (B).

4.5. Alterations in the number of CALR-immunostained cells

CALR-containing interneurons were scattered in the control hippocampus. They appeared in CA fields, mainly in the *stratum lacunosum-moleculare* (close to the hippocampal fissure), the *stratum radiatum*, *oriens*, and *pyramidale*. They were also present in the hilum of the DG, where they were located beneath the *stratum granulosum* (subgranular layer), in the centre of the hilum, and rarely between the GCs. Their dendrites and axons extended into the *stratum moleculare* and also formed a plexus in the hilum beneath the GCs. Strong CALR immunoreactivity was visible in the IML of DG: this CALR staining appeared to originate from

thin CALR-IR processes and was present in control (not shown) and PILO animals (Fig. 12A,C). The number of CALR-IR cells decreased significantly in the HF of PILO animals, although the decrease was less pronounced than that of PARV cells (Fig. 11B), which is in agreement with data from the subiculum already reported in the literature [141]. In a mouse (PILO1), the granular/subgranular layers expressed strong CALR-IR (Fig. 12A). CALR-stained cells were equally numerous in the ventral and dorsal blades of the *stratum granulosum/subgranulosum*. Morphologically, they appeared as average GCs that contained CALR in their cell bodies and proximal dendrites (Fig. 12B). Other epileptic animals (PILO2-9) showed CALR staining of thin varicose fibres in the hilum and IML close to GCs (Fig. 12C). Large multipolar neurons in the hilum (possibly MCs) were strongly stained with the CALR antibody in both control and PILO animals, according to the descriptions in the literature [142]. Higher magnification always revealed several thin-beaded neuronal processes strongly stained with CALR throughout the hilum and in the entire *stratum moleculare* (Fig. 12C). Statistical evaluation of the data revealed an approximately 30% significant decrease in the number of CALR-IR neurons in PILO animals compared to controls (Fig. 11B).

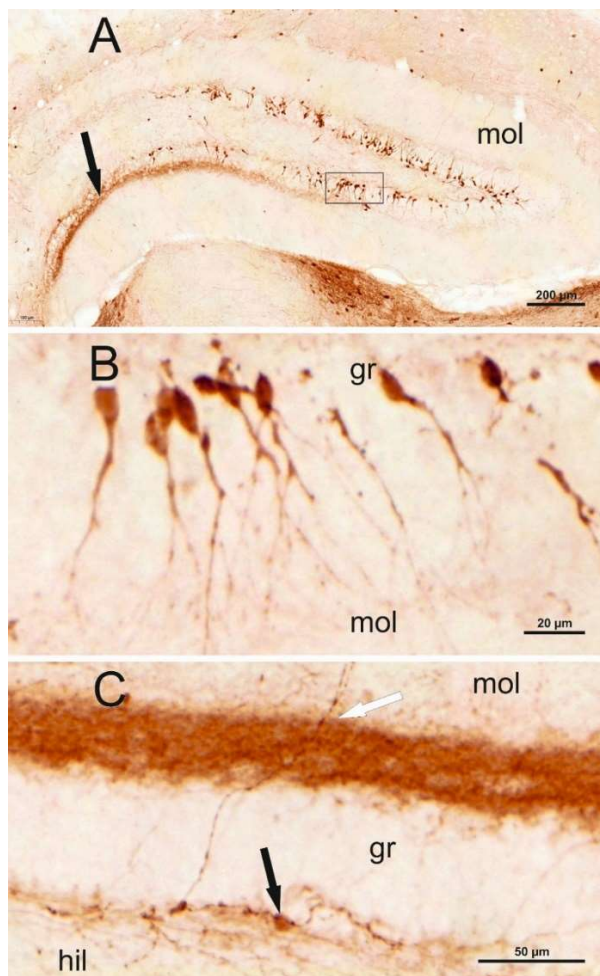


Figure 12. CALR staining in the PILO1 animal (A, B) and in PILO8 animal (C). Note the numerous CALR-IR GCs in the granular and subgranular layers in the DG of PILO1 (A). The arrow in PILO1 (A) points to IML, where strong CALR-IR cell processes are seen. The area delimited by a square (A) in PILO1 animal is shown with higher magnification in B. The CALR-stained IML is seen with higher magnification in PILO8 (C, white arrow). Note the scattered, varicose CALR-IR fibres in the hilum, and the *stratum granulosum* (B, C). The black arrow in the hilum is pointed at CALR-IR neuronal cell body (C). Abbreviations: **mol** = *stratum moleculare* of DG; **gr** = *stratum granulosum* of DG; **hil** = hilum of DG. Scale bars: 200 μm (A); 20 μm (B); 50 μm (C).

4.6. The impairment of spatial learning 3 months after SE

The effects of pilocarpine-evoked SE and chronic SRS episodes on spatial learning and memory capacities were tested in a Barnes maze, 3 months after pilocarpine treatment. In the Barnes maze, the control animals found the escape hole faster than the PILO mice on each trial occasion (Fig. 13). On day 3, a significant difference was detected between the two groups ($p = 0.043$). Control animals were also successful in the retrieval phase, the difference between the latencies of control and PILO mice during the probe trial was significant ($p = 0.025$). Spatial learning curves demonstrated that chronic seizures induced a marked decrease in learning, as well as in spatial memory performance (Table 5; Fig. 13). The effective learning process is demonstrated in controls by decreasing latencies, while PILO mice showed worse abilities (Fig. 13).

The following animals were the worst performers in the Barnes maze: PILO1, 4, 5, 8 (see also Table 4 for a comparison of neuronal loss). PILO1 and PILO4 had completely degenerated CA regions, PILO5 completely lost the CA3 region and also had cell loss in CA1 and in the hilum. PILO8 had patchy cell losses throughout CA1 and CA3 regions.

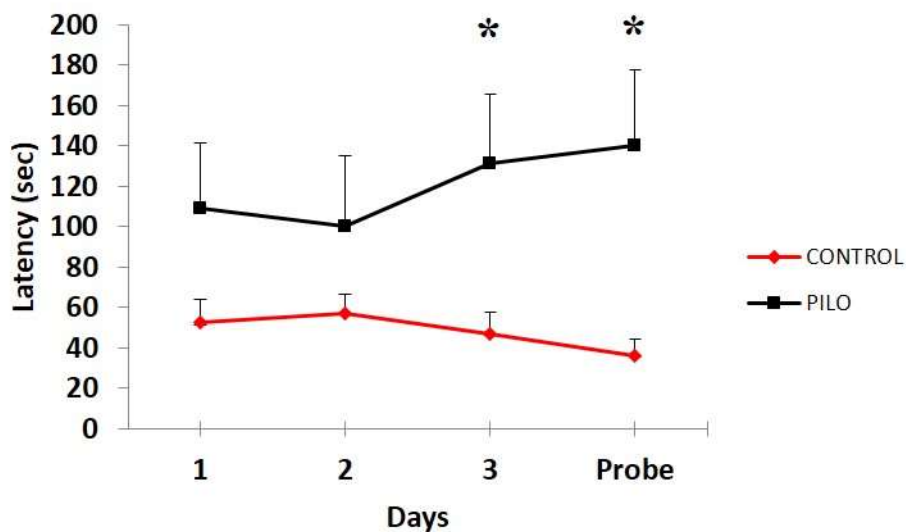


Figure 13. Performance of the control and PILO animals in the Barnes maze for four consecutive days. Two trials were performed on each day, except for the probe day. The average latencies of the control and PILO animals ($n = 9$ / groups) were plotted against time. The SEM values were depicted. The controls showed an improved performance as a function of time, whilst the performance of the PILO animals became worse. Using the paired t-test, the statistical analysis showed that the variances of the mean latencies in the two groups were significantly different on day 3 and day probe (* $p = 0.043$ and 0.025 , respectively).

4.7. A case report in pilocarpine-induced NMRI-strain epileptic mice

The animal PILO10 is presented below due to its histological uniqueness. This epileptic mouse was one of the first study. It survived only 3 months after SE, therefore this animal was not involved either in the statistical analyses of the IHC immunostainings or in the spatial learning test; however, we thought it was worth presenting this particular case.

The animal died one day before the Barnes maze test. This mouse was seriously ill, malnourished and showed strong SRS more times per day. During the observation time of that day, the animal had a severe seizure, which it did not survive. So instead of the usual perfusion, the brain was immediately removed and fixed by the immersion method to make it processable. As the IHC images reveal (Fig. 14), its hippocampus significantly degenerated, and the segments, layers, and sublayers of the HF could only be partially identified. Remarkably, despite such extensive neuronal loss, it survived for 3 months.

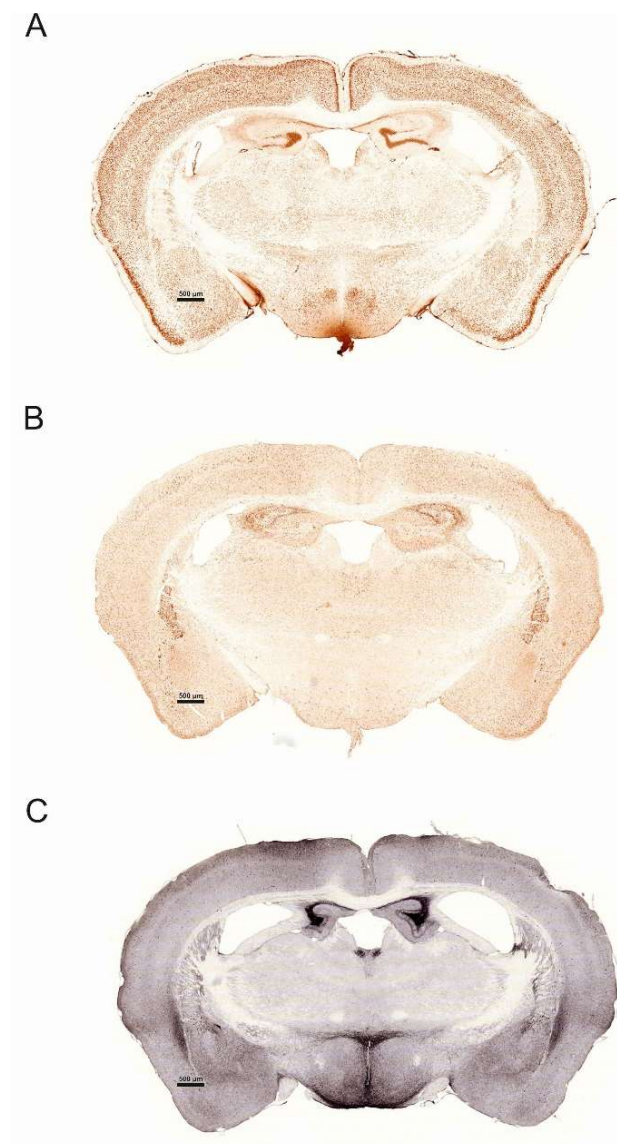


Figure 14. Representative images of the PILO10 hippocampus. Neuronal loss was detected by NeuN (A), microglial activation was revealed by Iba1 (B), and mossy fibre sprouting was attested by NPY immunostainings (C). Scale bars: 500 µm.

4.8. Effect of SZR104 on hippocampal microglial cells in pilocarpine-induced epileptic mice

In this study, we tested the effects of the synthetic KYNA analogue SZR104 - as a potential drug candidate in TLE - in pilocarpine-induced epilepsy model in mice. According to a previous study in rats [126] we suggested that SZR104 may have anticonvulsant properties and could potentially be beneficial in the treatment of seizures. Pretreatment with the KYNA analogue SZR104 failed to reduce the motor hyperactivity and SE in NMRI-strain mice. The animals, which were pretreated with SZR104 40 min before the pilocarpine injection (SZR104 + PILO group), presented similar symptoms: The latency of the onset of motor symptoms was not delayed, and severe tonic-clonic convulsions were not prevented by the KYNA analogue SZR104. Furthermore, SZR104 did not reduce pilocarpine-induced mortality. In contrast, controls receiving only the solvent of pilocarpine (0.9% NaCl) or saline and SZR104 injected alone caused neither symptoms nor mortality.

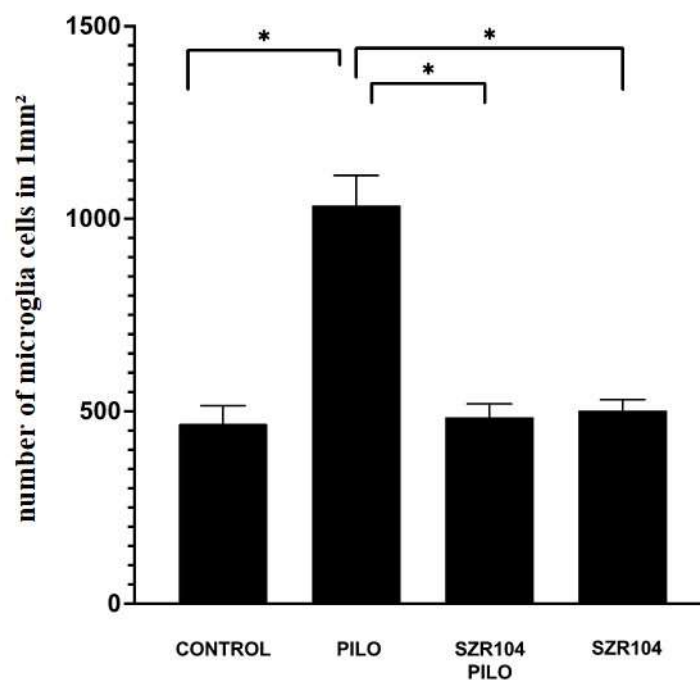


Figure 15. Analysis of Iba1-positive microglial cell counts in the entire HF of epileptic, and control mice (n = 4 sections / each animal; mean±SEM). Statistical differences were detected between the control, PILO, SZR104+PILO, and SZR104-treated animals (* $p < 0.05$).

Control mice displayed normal microglial cells. Iba1-stained cells were evenly distributed in the hippocampus, their shape and distribution were similar to those of the resting microglia. The diameter of the cell body was approximately 6-7 μm , and their ramified processes were thin and relatively short. The cells possessed 4-5 slender, 5-10 μm long processes (Fig. 16A).

Pilocarpine treatment induced a significant increase in the number of these cells when counted after 24 h and alteration of their phenotype. The number of Iba1-immunopositive cells in the hippocampal area of 1 mm² increased to ~1000 per mm² or greater, compared to the controls in which we counted ~500 cells or less in 1 mm² (Fig. 15).

In contrast, DAM cells reduce the complexity of their shape by retracting and thickening their branches [143]. The physiology of the microglia resulted in a more compact appearance of immunostaining for these cells. The area of the cells was larger in PILO mice. The diameters of the cell bodies were 8-12 μm , and the cytoplasmic processes were thicker compared to the cells of the resting microglia (Fig. 16B,C). The measured surface area of the cells increased significantly compared to the controls (Fig. 16E). While control, untreated microglial cell areas were in the $\leq 500 \mu\text{m}^2$ range, the cells from epileptic animals were significantly larger ($\leq 1500 \mu\text{m}^2$). SZR104 pretreatment prevented the microglial alterations caused by seizures. Both the number of Iba1-positive cells and the surface area of single cells remained close to the control values (Fig. 15, 16). When we compared the hippocampus of PILO animals to the hippocampus of the SZR104 + PILO group, the microglia-inhibitory effects of SZR104 proved to be significant (Fig. 15). Shape, size, and ramification were similar to the controls (Fig. 16D). The SZR104 administrated alone caused neither alterations in number of the microglial cells (Fig. 15) nor morphology and cell area. These were similar to the controls' (not shown).

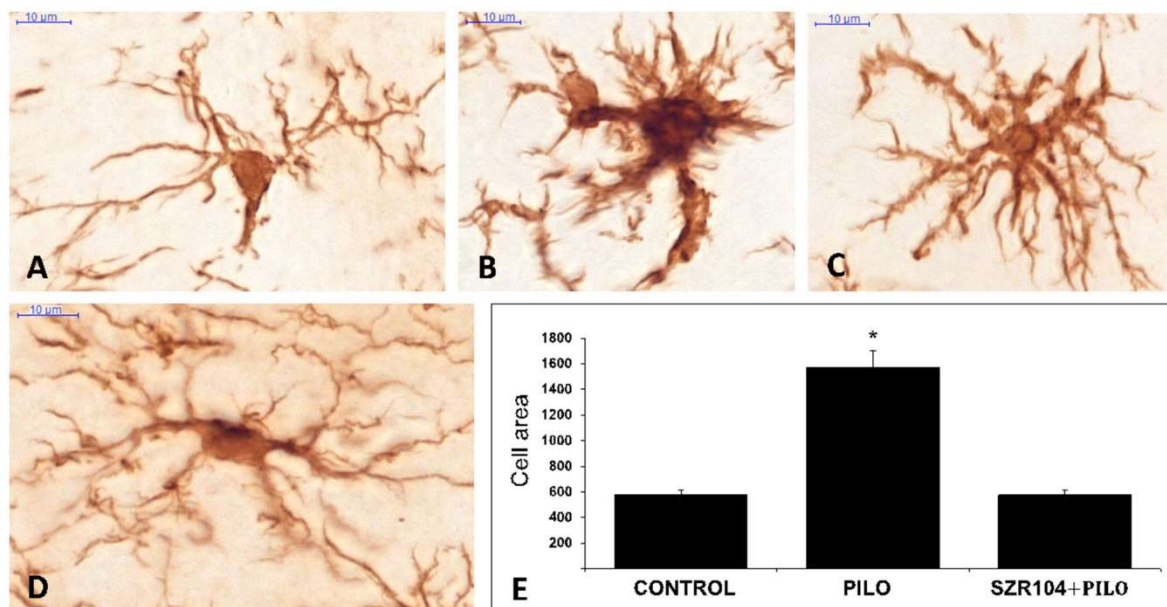


Figure 16. Iba1-stained microglial cells from control (A), PILO (B, C), and SZR104+PILO animals (D). The average microglial cell areas (cell body and processes) were depicted in μm^2 values on the y-axis ($n = 10$ cell / each group; mean \pm SEM) in the control, PILO, and SZR104+PILO animals (E), (* $p < 0.05$). Scale bar: 10 μm .

5. Discussion

In the present studies, we employed the established murine model of pilocarpine-induced epilepsy. In this model, we made novel observations regarding the long-term functional consequence on spatial learning and the neuropathological appearance of the sclerotised hippocampus. Moreover, using the same model, we identified an interesting novel short-term effect of the KYNA analogue SZR104 on activation and morphological changes in microglia. The major specific findings in the dorsal hippocampus are as follows:

- 1) Pilocarpine-induced high mortality due to SE and SRS in survivors persisted over the previously unassessed course of 3.5 months observation period in NMRI mice. Epileptic mice displayed severe disturbances of spatial learning and memory indicating the development of severe hippocampal dysfunction.
- 2) All animals developed severe HS characterised by severe neuronal damage that could culminate in the near-total destruction of the hippocampus, as shown by NeuN immunohistochemistry. Parallel to it, microglial cells are activated rapidly following pathological changes of the brain in epilepsy confirmed by Iba1 immunostaining. In addition, reactive sprouting of mossy fibres has been demonstrated using NPY immunohistochemistry. These findings are in accordance with previous data using shorter observation periods.
- 3) The specific loss of CALR-immunopositive and PARV-immunopositive interneurons in the hippocampus has also been confirmed in our model, moreover PARV-immunopositive astrocyte-like cells were novelly detected in the sclerotised hippocampus.
- 4) The potentially neuroprotective, novel KYNA analogue SZR104 did not reduce pilocarpine-induced seizures or seizure-induced mortality, however, it potently ameliorated the acute (24h) neuroinflammatory response detected by the Iba1-immunopositive microglial cell count and morphological changes.

The pilocarpin model has been one of the more widely used drug-induced chronic epilepsy models. Our findings confirm and further advance the understanding of the neuropathological features and pathomechanistic aspects of HS that are prominently developed in this model.

5.1. Learning and memory impairment caused by severe HS in epileptic mice

The degeneration of the hippocampus has also caused a significant deterioration in learning ability. Our experiments proved that spatial learning processes were slower during acquisition trials and spatial memory retrieval was significantly worse during the final probe process in epileptic versus control mice. This is in accordance with the literature data [144]. Similar (although less dramatic) impairment of spatial learning was observed after kainic acid lesions in the CA1 sector of the dorsal hippocampus in mice [144]. Nonepileptic experimental lesions of the dorsal and ventral hippocampus are also associated with impaired working memory and reference memory retrieval [145]. A similar spatial memory disturbance occurred after the lateral entorhinal cortex in our previous experiments [146]. The entorhinal cortex and the hippocampus are important in the spatial learning of rodents [146]. HS destroys not only the principal neurons but also several interneurons, and therefore reciprocal neuronal connections between the neocortex, entorhinal, and hippocampal cortices will be interrupted. In the present experiments, we detected HS in histological sections of the dorsal hippocampus. Neuronal loss in dorsal HF could well explain the spatial memory impairment seen in the Barnes maze experiments [144]. Similar results have been reported in epileptic C57BL/6 mice, where hippocampal neuronal loss was correlated with a significant increase in escape latency in the Morris water maze tests [147]. Neuronal loss in CA1, CA3, and the hilum was evaluated on thionin-stained sections of control and PILO animals 9 months after pilocarpine administration, and significant neuronal loss was found, which was correlated with the results of the Morris water maze [147]. We could also select the PILO animals with the worst learning and memory performance. However, further experiments are needed to accurately correlate the degree and location of neuronal loss, gliosis, and learning and memory performance. The correlation of HS and memory loss in our experiments was clinically significant, as hippocampus damage in human TLE has also been correlated with visuospatial memory loss in adult patients [138]. Hippocampal neurogenesis is also related to hippocampal-dependent learning, which we studied in this experiment. This assumption is consistent with the finding that when there is a deficit in the hippocampus, neurogenesis correlates with impaired spatial orientation and memory. The description of our observations on neurogenesis is discussed in section 5.3 of this chapter.

5.2. Neuronal loss, microglial activation and sprouting of mossy fibres in epileptic mice

In the present studies, cellular damage was detected in the *stratum pyramidale* and hilum of the hippocampal regions in the responding mice following SE (Fig. 17). Previous results show that

after pilocarpine-induced SE, the most sensitive hilar neurons are damaged first, followed by damage to neurons in the *stratum pyramidale* of the CA regions by day four [91]. Neuronal loss in the Ammon's horn was approximately 50%, while in the DG it was slightly less, around 30% compared to the control. There are several possible causes of neuronal damage during convulsions. Enhanced transmitter release is detected in increased excitation caused by SE, in particular high level of Glu, which causes severe neuronal damage in two steps [10, 25, 148]. Acute cerebral edema develops first due to the influx of ions and water through the ion channels kept open by excitatory transmitters (this process is non-selective because all hyperexcitable cells are affected) [10, 25, 149]. Most of the cells are still able to compensate for this change through their ATP-dependent ion transporters and pump out the excess water and ions; however, the most sensitive hilar interneurons are destroyed early in this oedematous phase. Subsequent damage is already a delayed Ca-mediated process [10, 149]. Ca^{2+} influx through channels opened by voltage-dependent NMDA-type Glu receptors acts as a signal and releases additional Ca^{2+} from cell stores to flood the intracellular space. This elevated Ca^{2+} concentration acts by activating degradative enzymes [150] (cellular energy production, mitochondria and cytoskeleton, DNA pool, and axon transport are affected). Activation of the caspase family of enzymes leads to apoptosis [151]. Previous experiments have shown a significant reduction in the number of neurons in the *stratum pyramidale* of CA3 as early as day four after the onset of SE.

Neuronal damage is a consequence of acute SE [102, 119, 152, 153]. Hypoxic conditions develop in the brain parenchyma during SE, where despite the increase in regional cerebral blood flow, neurons are deprived of oxygen [153]. Due to the extracellular accumulation of Glu, potassium, hydrogen carbonate, and ammonia, the astrocytes swell, obliterate the extracellular space, and hinder the diffusion of nutrients. Neurons are deprived of nutrients, and this condition, together with hypoxia leads to cell damage and necrosis [152, 153]. These processes, which lead to acute neuronal cell death, are well documented in the literature [152-154]. Neuronal degeneration in the hippocampus was clearly demonstrated in our present studies with NeuN immunohistochemistry. PILO mice demonstrated the doctrine of graded sensitivity of the hippocampal subfields [154]. CA1 and CA3 were the areas where the pyramidal layer was mainly affected. According to neuronal loss, the cross-sectional area of HF decreased significantly, as measured in our experiments. This HF shrinkage is regularly observed in MTLE in human patients [155].

There are several views on the vulnerability of hippocampal neurons. According to Sloviter [111] the first step is the destruction of MCs leading to synaptic reorganisation. He is credited

with the hypothesis of sleeping basket cells, which suggests that the death of stimulatory MCs leads to a reduction in the function of inhibitory basket cells. In a contradictory finding, Scharfman [40] argues that primarily inhibitory interneurons are damaged while MCs survive SE. This indicates that there are probably multiple populations of MCs and that they are differentially susceptible in epilepsy.

Although the neurons degenerate the most, however, astroglial cells are also affected, resulting in the death of more neurons as a consequence. In general, glial cell activation is a secondary phenomenon in SE that facilitates tissue reorganisation [156, 157]. In contrast, Kang TC argues that neuronal death alone is not a sufficient condition for the development of SE [158]. In their experiments, they have already shown astroglial damage on day one, i.e., it precedes neuronal degeneration. Because of their important role in nourishing neurons and eliminating their breakdown products, they affect neuronal transmission, their destruction makes neurons more vulnerable and also predisposes them to apoptosis or necrosis.

Microglial cells are thought to be the most important immunocompetent cell type in the brain and the main regulator of inflammatory processes in the brain. Microglial cells are rapidly activated following pathological changes in the brain in epilepsy [92]. The widespread expression of neurotransmitter receptors in microglial cells renders cells sensitive to neuronal hyperactivity. These receptors initiate the transformation of the microglial cell and also regulate its cytokine secretion [134]. Microglia can promote neurodegeneration [130] but can also be a protective device by detecting damage and also exerting a protective role in neurodegeneration. Our experiments clearly pointed to this role. DAM cells were seen in the layers that suffered massive neuronal loss (Fig. 17). This phenomenon points to the possibility that DAM occupied the sclerotic hippocampus subfields to maintain a kind of homeostasis after the death of neurons. However, this hypothesis must be validated by immunohistochemical detection of DAM markers [132].

Recent research has shown that microglia mediate forgetting via complement-dependent synaptic elimination [159]. This indicates that the role of microglial cells in the brain is more complex than previously thought. It opens a new direction for researchers in experiments on learning and forgetting.

The sprouting of mossy axons in epilepsy is well documented not only in experimental animals [94, 98, 108, 160] but also in the human brain [93, 161]. The main layers targeted by the sprouting axons are the *stratum moleculare* of the DG, the hilum of the DG, and the *stratum lucidum* of CA3 [94, 98, 108, 160, 161]. Other locations where the sprouted axons terminate are the infrapyramidal sublayer of the CA3 *stratum oriens*, and the *stratum granulosum*, and

the IML of the DG [161]. We detected the sprouting with NPY immunohistochemistry and observed the ectopic axons even in the case of complete loss of the principal neurons in the area corresponding to the *stratum lucidum* of CA3. This observation indicates that these sprouted axons persisted without postsynaptic targets. They probably released NPY, and the released peptide exerted its antiepileptic effect through diffusion to the DG. The increase in NPY expression was detected in GCs by immunohistochemistry [162] and *in situ* hybridisation [163], demonstrating the alteration of the GC phenotype in epilepsy [163]. NPY causes depression of epileptiform activity of the GCs [164]. The sprouting plays an important role in hippocampus reorganisation, and it is a standard feature of human HS in TLE [93, 161].

The strong increase in NPY expression proved that in HS, the peptidergic component of hippocampal neurotransmission survived better than the Glu system. This could possibly lead to alterations in synaptic transmission of the hippocampal cortex. Instead of fast Glu signaling, slow metabotropic peptidergic signaling prevailed. The slowdown of signaling could also contribute to the worsening of learning and memory functions.

5.3. Specific loss of PARV-immunopositive and CALR-immunopositive interneurons in epileptic mice

Neurons containing Ca-binding proteins (PARV, CARL, and CALB) are more resistant to SE. These proteins reduce the increase in intracellular Ca^{2+} levels and thus protect against the activation of degenerative degradative enzymes. A large population (approximately 50%) of the hippocampal PARV-containing GABAergic neurons was lost in HS (Fig. 17). The PARV-containing interneurons of HF are located mainly in the PC and GC layers, and the hilum [56]. They are mainly GABAergic basket cells and axo-axonic cells that exert inhibition on cell bodies, proximal dendrites, and initial axon segments [56]. The number of these neurons decreased significantly in the sclerosed hippocampi in our experiments, indicating a decrease in inhibition in the *stratum pyramidale* and *stratum granulosum*, as documented by the literature data [56, 100, 101]. Similar observations have been described in experimental rats with absence epilepsy [165] and kindling epilepsy [166]. Degeneration in the *stratum pyramidale* swept out not only the principal cells but also PARV-IR GABAergic cells. We encountered only very few PARV-IR cell bodies (3-4 in total), located close to the alveus and in the subiculum. Data from the literature support this observation [101, 155, 167]. The presence of scattered PARV-IR astrocytes in the sclerosed regions is a new finding. Up-regulation of PARV in reactive astrocytes and ependymal cells was described *in vivo* [168] and *in vitro* [169]. Up-regulation was caused by brain injury [168] and virus infection [169]. In these experiments, the up-

regulation of PARV was discussed in connection with changes in cell metabolism and proliferation signaling [168, 169]. In our experiments, microenvironment alterations due to neurodegeneration and axonal sprouting could be the explanation for the expression of astrocytic PARV expression. However, this issue needs to be examined in further experiments with immunostainings using PARV antibodies and specific astrocyte markers.

We also describe the degeneration of CALR-containing interneurons in the epileptic hippocampus (Fig. 17). This decrease was approximately 30% in terms of the total number of cells/mm². The expression of CALR in the GCs could be explained by the phenotype changes of these neurons in epilepsy [163]. This statement needs some clarifications:

According to the literature, neurogenesis is accelerated in epilepsy and, as a consequence, after pilocarpine treatment. In adults, neurogenesis is observed in only a few areas of the brain, and DG is one of them. A study shows neurogenesis within the adult hippocampus (under physiological conditions and in depression) [170]. The progenitor cells are located in the subgranular layer, from which they proliferate, differentiate, and migrate to the *stratum granulosum* (mainly into its inner zone). This was also observable in our sections. There are three different types among these cells (Type 1,2,3). Type 3 progenitor cells are CALR-positive. The presence of these identified cells is also detectable in a control animal (control 1 is very similar to PILO1 in this layer), therefore we think that there can be progenitor cells among CALR-IR cells. This hypothesis should be supported by subsequent specific immunohistochemical staining, possibly double staining. BrdU (thymidine analogue 5'-bromo-2'-deoxyuridine) indicates that all cells are in S phase. If this is combined with doublecortin (DCX) or Neuro D labelling, we have a good chance of differentiate these cells. DCX-labelled cells belong to the neuronal lineage. These cells can belong to the population of late mitotic neuronal progenitor cells or early postmitotic immature neurons. Since Neuro D is a marker for early cells of the neuronal lineage it could be used to answer the dilemma described above. It is expressed during neurogenesis in adult DG in the subgranular zone and in the inner layer of the *stratum granulosum* [171].

MCs also express CALR in normal and epileptic mice, and their number decreases in epileptic animals, as shown in the literature [142]. The decrease in other hippocampal CALR-IR cells is probably related to HS. The degeneration of the principal neurons (which are synaptic targets of the interneurons) is accompanied by the degeneration of the interneurons, as in the case of PARV-IR cells. These observations about the decrease are supported by the data in the literature [166, 172]. Similarly, a decrease in CALR-IR cells in DG was observed in the dorsal hippocampus in kindling rat experiments [166]. On the other hand, a significant increase in the

number of CALR-IR Cajal - Retzius cells was detected in epileptic human brain samples [173, 174]. The sprouting of CALR-IR nerve fibres of DG was also noted in human HS [93]. Our present observations on the abundance of thin CALR-IR fibres in the DG in epileptic mice support the possible participation of CALR-IR neurons in the sprouting and reorganisation of the DG in HS.

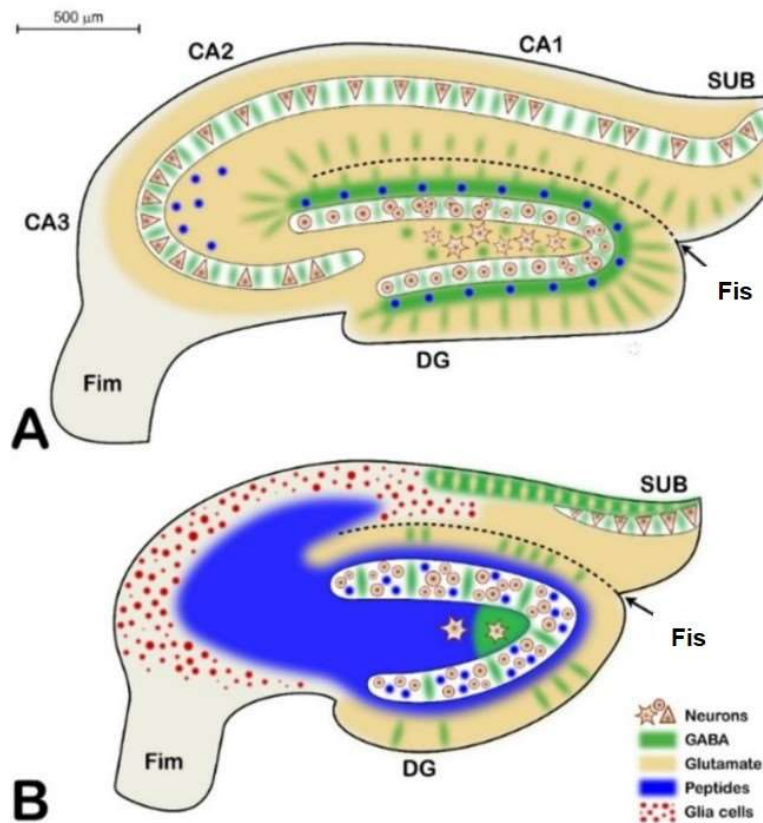


Figure 17. Scheme of the neurochemical parcellation of the hippocampus in the control (A) versus PILO (B) animals. Principal neurons are represented by triangular, circular, and multipolar shapes. GABAergic transmission is depicted in green, Glu transmission is beige, and peptide transmitters are in blue. Glia is represented by red dots. The PILO hippocampus was not only shrunk, but also invaded by peptidergic axons, some of which did not have postsynaptic cells, and the peptide released was diffusing toward unknown targets. This neurochemical alteration drastically changed the function of the hippocampus, as it was shown by the Barnes maze experiments. Abbreviations: CA1, CA2, and CA3 are the regions of the *cornu ammonis*; DG = dentate gyrus; SUB = subiculum; Fim = fimbria; Fis = hippocampal fissure; Scale bar: 500 μm.

In conclusion, although the decrease of CALR-IR cells in PILO mice was significant compared to the control, it was still less than that of PARV-IR cells. This may be influenced by the fact that CALR staining alone can not differentiate CALR-IR interneurons from the neurogenesis-affected cells that are also labelled with CALR. However, this ambiguity of CALR-IR neurons in epilepsy needs to be further investigated.

5.4. SZR104 effect on changes in number and phenotype of microglial cells in pilocarpine-induced epileptic mice

Microglial cells are activated rapidly following pathological changes in the brain [129].

Our experiments also proved that the acute microglial response in PILO mice was very pronounced and that this activation was conspicuously inhibited by the synthetic kynurenic acid analogue SZR104. The precise mechanism and significance of this inhibition remain unclear, but nevertheless it may signal a yet unexplored mechanism that can target neuroinflammation in response to neuronal injury induced by epileptic seizures or SE. [136].

In microglial cells, the expression of neurotransmitter receptors on their surface renders them sensitive to neuronal hyperactivity [132-134, 175]. The activation of these receptors may initiate the transformation of microglia from resting to their activated status by simultaneously regulating their cytokine secretion [132-134, 175, 176].

The microglial activation usually is peaking ~5-7 days following CNS injury [177]. However, in our experiments, the developing SRS comprise not a single injury, but a series of recurrent spasms resulting in an ongoing neurodegeneration. The increased number of DAM is detectable in Iba1-stained sections even months later after pilocarpine treatment. In the long term microglia can promote either neurodegeneration [130-132] or even neuroprotection [131, 132]. Currently, it is unclear whether the acute changes observed in microglia in the present study are beneficial or destructive, although the almost complete neurodegeneration observed in the later timepoints suggests the latter [131, 132]. Parallel *in vitro* studies confirmed that SZR104 can also inhibit lipopolysaccharide-induced phagocytosis in cultured microglial cells, and the inhibitory action of SZR104 was thought to be mediated perhaps through the activation of the aryl hydrocarbon receptor, a known intracellular target of KYNA. Further experiments are necessary to elucidate both the exact role of microglia over the time course of our HS model and the molecular target of SZR104 or related KYNA analogues.

6. Conclusions

The most important novel findings in our studies were the following:

1. Pilocarpine-induced chronic epilepsy in NMRI mice is an excellent preclinical model of chronic TLE that can simulate all the major features of the human pathology. This includes severe hippocampal dysfunction and structural alterations.
2. The novel long-term observation period enables the detection of large-scale neuronal loss including both principal neurons and selected populations of GABAergic interneurons, reactive axonal sprouting, and microglial activation, all the hallmarks of severe HS.
3. SZR104 was shown to selectively ameliorate the acute microglial response, suggesting the involvement of kynurenine metabolites in this response.

Acknowledgements

First of all, I would like to express my deepest gratitude to my family and friends, for their emotional support, unconditional love, tolerance, and for always being there for me. Thank you for accepting lost evenings, weekends, and holidays.

Officially, I would like to thank my supervisor, Prof. Dr. András Mihály, who provided me the opportunity to join his research group and gave access to the laboratory and research facilities. I would like to express my special thanks to Prof. Dr. Antal Nógrádi, the head of the Department of Anatomy, Histology, and Embryology, for supporting to finish my PhD thesis.

I would like to thank the following two people without whom this thesis would not have been possible. I would like to express my deepest gratitude to Dr. Emőke Borbély, whose support, generous help, and friendship were essential to the completion of my doctoral work and PhD thesis over the past years. I wish to express my sincere and heartfelt gratitude to Dr. Ferenc Domoki for his personal guidance, professional advice and, even more importantly, for his patience, continuous support, and encouragement.

I owe a debt of gratitude to Prof. Dr. Ferenc Bari for his kind support and believing me all the time during this long journey.

Special thanks go to Mónika Kara for her technical assistance during the experiments, and to Dr. Endre Dobó for his guidance in the laboratory work.

I must mention my former teachers, who have played an immense role in bringing me to this point. First of all, I would like to mention Zsuzsanna Berzai Trencséniné, my former high school teacher of biology and chemistry. She made me fall in love with these two subjects and eventually I got my degree as a result at the Attila József University. I have also had the pleasure of meeting some excellent professors of the university who have set an example both professionally and as people. I would like to thank Prof. Dr. Éva Fekete, Prof. Dr. Katalin Halasy, Prof. Dr. József Toldi, Prof. Dr. Csaba Visy, Dr. Irma Tari Dr. Miklósné Görgényi, Dr. Mária Simon Dr. Lehoczkiné, Prof. Dr. István Hannus, Prof. Dr. Gyula Farkas, and Dr. Zoltán Galbács for their dedicated work, from whom I have learnt a lot.

I also would like to thank my colleagues who have supported me in any way during my work. Last but not least, a special thanks goes to all the mice who gave their lives for my PhD.

*This study was supported by grants from the Ministry of National Resources (**GINOP-2.3.2-15-2016-00034**) through the European Union Cohesion Fund.*

Bibliography

1. https://www.who.int/news-room/fact-sheets/detail/epilepsy/?gad_source=1&gclid=EAIaIQobChMI76jPtOLnhQMVnliRBR2hoQW5EAAYASAAEgLFpFD_BwE.
2. Walker, W.H.S.a.M.C., ed. *ABC of Epilepsy*. First Edition ed. ABC series. 2012, Blackwell Publishing Ltd.: UK. 1-13.
3. Jerome Engel, J., Timothy A. Pedley, ed. *Epilepsy: A comprehensive textbook*. 2nd ed. Vol. I. 2008, Lippincott Williams & Wilkins: Philadelphia, USA.
4. Richard E Appleton, A.N., David W Chadwick, James M MacKenzie, David F Smith, ed. *Atlas of Epilepsy*. Second edition ed. 2007, Informa UK Ltd. 7-96.
5. Curia, G., et al., *The pilocarpine model of temporal lobe epilepsy*. J Neurosci Methods, 2008. **172**(2): p. 143-57.
6. Fabene, P.F., et al., *Structural and functional MRI following 4-aminopyridine-induced seizures: a comparative imaging and anatomical study*. Neurobiol Dis, 2006. **21**(1): p. 80-9.
7. Hungarian Epilepsy League, M.o.H., *Ministry of Health professional guidelines on the recognition, treatment and care of epileptic seizures and epilepsy*. 2010, Health Gazette.
8. Péntek M, B.D., Gulácsi L, Mikudina B, Arányi Z, Juhos V, Baji P, Brodsky V., *Survey of adults living with epilepsy in Hungary: health-related quality of life and costs*. Hungarian Neurology Review, 2013. **66**(7-8): p. 251-61.
9. Szirmai, I., ed. *Neurology*. 2011, Medicina Könyvkiadó Rt.,: Budapest
10. Olney, J.W., R.C. Collins, and R.S. Sloviter, *Excitotoxic mechanisms of epileptic brain damage*. Adv Neurol, 1986. **44**: p. 857-77.
11. J., N., *Questions of epileptogenesis and prevention in symptomatic epilepsies*. Hungarian Neurology Review, 2004(57(5-6):): p. 164-73.
12. Kamondi, A., et al., *Epilepsy and epileptiform activity in late-onset Alzheimer disease: clinical and pathophysiological advances, gaps and conundrums*. Nat Rev Neurol, 2024. **20**(3): p. 162-182.
13. Mumenthaler, M., ed. *Neurológia*. 1996, Medicina Könyvkiadó Rt.: Budapest.
14. Epilepsy, I.L.A., ed. *Commission on Classification and Terminology of the International League Against Epilepsy*. 1981.
15. Engel, J., Jr., *Introduction to temporal lobe epilepsy*. Epilepsy Res, 1996. **26**(1): p. 141-50.
16. Ozkara, C., et al., *Memory in patients with drug-responsive mesial temporal lobe epilepsy and hippocampal sclerosis*. Epilepsia, 2004. **45**(11): p. 1392-6.
17. Harvey, A.S., et al., *Febrile seizures and hippocampal sclerosis: frequent and related findings in intractable temporal lobe epilepsy of childhood*. Pediatr Neurol, 1995. **12**(3): p. 201-6.
18. Maher, J. and R.S. McLachlan, *Febrile convulsions. Is seizure duration the most important predictor of temporal lobe epilepsy?* Brain, 1995. **118 (Pt 6)**: p. 1521-8.
19. Halasz, P. and A. Fogarasi, *[Temporal lobe epilepsy--state of art review]*. Ideggyogy Sz, 2006. **59**(9-10): p. 331-52.
20. Engel J Jr, W.S., French J, Sperling M, Williamson P, Spencer D, Gumnit R, Zahn C, Westbrook E, Enos B;, *Practice parameter: temporal lobe and localized neocortical resections for epilepsy*. Neurology, 2003(60(4)): p. 538-47.
21. Jackson, G.D., et al., *Hippocampal sclerosis studied in identical twins*. Neurology, 1998. **51**(1): p. 78-84.

22. Michelson, H.B. and E.W. Lothman, *An in vivo electrophysiological study of the ontogeny of excitatory and inhibitory processes in the rat hippocampus*. Brain Res Dev Brain Res, 1989. **47**(1): p. 113-22.
23. Schwann J, M.L., ed. *Developmental issues in animal models*. Epilepsy: A comprehensive textbook, ed. P.T. Engel J Jr. 1997, Lippincott-Raven: Philadelphia. 467-79.
24. Falconer, M.A., E.A. Serafetinides, and J.A. Corsellis, *Etiology and Pathogenesis of Temporal Lobe Epilepsy*. Arch Neurol, 1964. **10**: p. 233-48.
25. Meldrum, B.S., *Cell damage in epilepsy and the role of calcium in cytotoxicity*. Adv Neurol, 1986. **44**: p. 849-55.
26. Amaral, D.G., *Memory: Anatomical Organization of Candidate Brain Regions*, in *Handbook of Physiology: The Nervous System*, B.F. Mountcastle VB, Geiger SR, Editor. 1987, American Physiological Society, Bethesda: Maryland.
27. Swanson, L.W., Köhler, C., & Björklund, A., *The limbic region. I: The septohippocampal system.*, in *Handbook of chemical neuroanatomy, Integrated systems of the CNS, Part I*, H.T. Björklund A., Swanson L.W., Editor. 1987, Elsevier: Amsterdam. p. pp. 125-277.
28. Amaral, D.G., N. Ishizuka, and B. Claiborne, *Neurons, numbers and the hippocampal network*. Prog Brain Res, 1990. **83**: p. 1-11.
29. Saladin, K.S., *Anatomy & Physiology: The Unity of Form and Function*. 2012: McGraw-Hill.
30. Filimonoff, I.N., *A rational subdivision of the cerebral cortex*. Arch Neurol Psychiatry, 1947. **58**(3): p. 296-311.
31. Amaral, D.G., *Emerging principles of intrinsic hippocampal organization*. Curr Opin Neurobiol, 1993. **3**(2): p. 225-9.
32. Amaral, D., & Lavenex, P., ed. *Hippocampal neuroanatomy*. The hippocampus book, ed. R.M. P. Andersen, D. Amaral & T. Bliss & J. O'Keefe. 2007, Oxford University Press. pp. 37-114.
33. Halasy, K., *Neuroanatomical characterization of inhibitory interneurons and their connections in rat hippocampal formation*, in *Faculty of Veterinary Sciences*. 2000, Saint Stephen's University: Budapest. p. 3-41.
34. Hjorth-Simonsen, A. and B. Jeune, *Origin and termination of the hippocampal perforant path in the rat studied by silver impregnation*. J Comp Neurol, 1972. **144**(2): p. 215-32.
35. Hjorth-Simonsen, A. and S. Laurberg, *Commissural connections of the dentate area in the rat*. J Comp Neurol, 1977. **174**(4): p. 591-606.
36. Lorente De Nó, R., *Studies on the structure of the cerebral cortex. II. Continuation of the study of the ammonic system*. Journal für Psychologie und Neurologie, 1934. **46**: p. 113-177.
37. H, S., *Allocortex*. 1975, Heidelberg, New York: Springer.
38. Zs, M., *A hippocampális neuronhálózatok átalakulása krónikus temporális lebeny epilepsziában*, in *A hippocampus mint közös patológiai tényező egyes neuropszichiátriai kórképekben*, P. Halász, Editor. 2005, Melinda Kiadó: Budapest. p. pp. 61-101.
39. Sloviter, R.S., et al., *"Dormant basket cell" hypothesis revisited: relative vulnerabilities of dentate gyrus mossy cells and inhibitory interneurons after hippocampal status epilepticus in the rat*. J Comp Neurol, 2003. **459**(1): p. 44-76.
40. Scharfman, H.E., et al., *Survival of dentate hilar mossy cells after pilocarpine-induced seizures and their synchronized burst discharges with area CA3 pyramidal cells*. Neuroscience, 2001. **104**(3): p. 741-59.

41. Mihály, A., *Anatomia Essentialis III*. Vol. 1. 2006, Szeged: University of Szeged. 136,154.
42. Griffith, W.H., T.H. Brown, and D. Johnston, *Voltage-clamp analysis of synaptic inhibition during long-term potentiation in hippocampus*. J Neurophysiol, 1986. **55**(4): p. 767-75.
43. Ashwood, T.J., B. Lancaster, and H.V. Wheal, *Intracellular electrophysiology of CA1 pyramidal neurones in slices of the kainic acid lesioned hippocampus of the rat*. Exp Brain Res, 1986. **62**(1): p. 189-98.
44. Dingledine, R., A.A. Roth, and G.L. King, *Synaptic control of pyramidal cell activation in the hippocampal slice preparation in the rat*. Neuroscience, 1987. **22**(2): p. 553-61.
45. Miles, R. and R.K. Wong, *Inhibitory control of local excitatory circuits in the guinea-pig hippocampus*. J Physiol, 1987. **388**: p. 611-29.
46. Stanton, P.K. and T.J. Sejnowski, *Associative long-term depression in the hippocampus induced by hebbian covariance*. Nature, 1989. **339**(6221): p. 215-8.
47. Buzsáki, G., *Feed-forward inhibition in the hippocampal formation*. Prog Neurobiol, 1984. **22**(2): p. 131-53.
48. Somogyi, P., et al., *Identified axo-axonic cells are immunoreactive for GABA in the hippocampus and visual cortex of the cat*. Brain Res, 1985. **332**(1): p. 143-9.
49. Ribak, C.E., J.E. Vaughn, and K. Saito, *Immunocytochemical localization of glutamic acid decarboxylase in neuronal somata following colchicine inhibition of axonal transport*. Brain Res, 1978. **140**(2): p. 315-32.
50. Kohler, C., V. Chan-Palay, and J.Y. Wu, *Septal neurons containing glutamic acid decarboxylase immunoreactivity project to the hippocampal region in the rat brain*. Anat Embryol (Berl), 1984. **169**(1): p. 41-4.
51. Freund, T.F. and M. Antal, *GABA-containing neurons in the septum control inhibitory interneurons in the hippocampus*. Nature, 1988. **336**(6195): p. 170-3.
52. Pelkey, K.A., et al., *Hippocampal GABAergic Inhibitory Interneurons*. Physiol Rev, 2017. **97**(4): p. 1619-1747.
53. Schwartzkroin PA, M.A., *Electrophysiology of hippocampal neurons*, in *Cerebral Cortex. Further aspects of cortical function, including hippocampus*, P.A. Jones EG, Editor. 1987, Plenum Press: New York. p. pp. 295-343.
54. Lopes da Silva, F.H., et al., *Anatomic organization and physiology of the limbic cortex*. Physiol Rev, 1990. **70**(2): p. 453-511.
55. Buzsáki, G. and J.J. Chrobak, *Temporal structure in spatially organized neuronal ensembles: a role for interneuronal networks*. Curr Opin Neurobiol, 1995. **5**(4): p. 504-10.
56. Freund, T.F. and G. Buzsáki, *Interneurons of the hippocampus*. Hippocampus, 1996. **6**(4): p. 347-470.
57. Dingledine, R. and L. Gjerstad, *Reduced inhibition during epileptiform activity in the in vitro hippocampal slice*. J Physiol, 1980. **305**: p. 297-313.
58. Schwartzkroin, P.A. and D.A. Prince, *Changes in excitatory and inhibitory synaptic potentials leading to epileptogenic activity*. Brain Res, 1980. **183**(1): p. 61-76.
59. Herron, C.E., R. Williamson, and G.L. Collingridge, *A selective N-methyl-D-aspartate antagonist depresses epileptiform activity in rat hippocampal slices*. Neurosci Lett, 1985. **61**(3): p. 255-60.
60. Dingledine, R., M.A. Hynes, and G.L. King, *Involvement of N-methyl-D-aspartate receptors in epileptiform bursting in the rat hippocampal slice*. J Physiol, 1986. **380**: p. 175-89.
61. Freund, T.F., et al., *Serotonergic control of the hippocampus via local inhibitory interneurons*. Proc Natl Acad Sci U S A, 1990. **87**(21): p. 8501-5.

62. Freund, T.F., *GABAergic septal and serotonergic median raphe afferents preferentially innervate inhibitory interneurons in the hippocampus and dentate gyrus*. *Epilepsy Res Suppl*, 1992. **7**: p. 79-91.
63. Gall, C., et al., *Localization of enkephalin-like immunoreactivity to identified axonal and neuronal populations of the rat hippocampus*. *J Comp Neurol*, 1981. **198**(2): p. 335-50.
64. Loren, I., et al., *Distribution of vasoactive intestinal polypeptide in the rat and mouse brain*. *Neuroscience*, 1979. **4**(12): p. 1953-76.
65. Sims, K.B., et al., *Vasoactive intestinal polypeptide (VIP) in mouse and rat brain: an immunocytochemical study*. *Brain Res*, 1980. **186**(1): p. 165-83.
66. Handelmann, G., et al., *CCK-containing terminals in the hippocampus are derived from intrinsic neurons: an immunohistochemical and radioimmunological study*. *Brain Res*, 1981. **224**(1): p. 180-4.
67. Greenwood, R.S., et al., *Cholecystokinin in hippocampal pathways*. *J Comp Neurol*, 1981. **203**(3): p. 335-50.
68. Somogyi, P., et al., *Different populations of GABAergic neurons in the visual cortex and hippocampus of cat contain somatostatin- or cholecystokinin-immunoreactive material*. *J Neurosci*, 1984. **4**(10): p. 2590-603.
69. Morrison, J.H., et al., *Immunohistochemical distribution of pro-somatostatin-related peptides in hippocampus*. *Neurosci Lett*, 1982. **34**(2): p. 137-42.
70. Köhler C, C.-P.V., *Somatostatin-like immunoreactive neurons in the hippocampus: an immunocytochemical study in the rat*. *Neurosci Letters*, 1982 Dec 31: p. 34 (3) pp.259-64.
71. Finsen, B.R., et al., *Somatostatin and neuropeptide Y in organotypic slice cultures of the rat hippocampus: an immunocytochemical and in situ hybridization study*. *Neuroscience*, 1992. **47**(1): p. 105-13.
72. Baimbridge, K.G. and J.J. Miller, *Immunohistochemical localization of calcium-binding protein in the cerebellum, hippocampal formation and olfactory bulb of the rat*. *Brain Res*, 1982. **245**(2): p. 223-9.
73. Buchan, A.M. and K.G. Baimbridge, *Distribution and co-localization of calbindin D28k with VIP and neuropeptide Y but not somatostatin, galanin and substance P in the enteric nervous system of the rat*. *Peptides*, 1988. **9**(2): p. 333-8.
74. Gulyas, A.I., et al., *Calretinin is present in non-pyramidal cells of the rat hippocampus-I. A new type of neuron specifically associated with the mossy fibre system*. *Neuroscience*, 1992. **48**(1): p. 1-27.
75. Ben-Ari, Y., *Brain damage caused by seizure activity*. *Electroencephalogr Clin Neurophysiol Suppl*, 1987. **39**: p. 209-11.
76. Represa, A., E. Tremblay, and Y. Ben-Ari, *Sprouting of mossy fibers in the hippocampus of epileptic human and rat*. *Adv Exp Med Biol*, 1990. **268**: p. 419-24.
77. Sloviter, R.S., *Status epilepticus-induced neuronal injury and network reorganization*. *Epilepsia*, 1999. **40 Suppl 1**: p. S34-9; discussion S40-1.
78. Ben-Ari, Y., *Cell death and synaptic reorganizations produced by seizures*. *Epilepsia*, 2001. **42 Suppl 3**: p. 5-7.
79. Tauck, D.L. and J.V. Nadler, *Evidence of functional mossy fiber sprouting in hippocampal formation of kainic acid-treated rats*. *J Neurosci*, 1985. **5**(4): p. 1016-22.
80. Magloczky, Z., et al., *Changes in the distribution and connectivity of interneurons in the epileptic human dentate gyrus*. *Neuroscience*, 2000. **96**(1): p. 7-25.
81. Lehmann, T.N., et al., *Alterations of neuronal connectivity in area CA1 of hippocampal slices from temporal lobe epilepsy patients and from pilocarpine-treated epileptic rats*. *Epilepsia*, 2000. **41 Suppl 6**: p. S190-4.

82. Babb, T.L., *Synaptic reorganizations in human and rat hippocampal epilepsy*. Adv Neurol, 1999. **79**: p. 763-79.
83. Margerison, J.H. and J.A. Corsellis, *Epilepsy and the temporal lobes. A clinical, electroencephalographic and neuropathological study of the brain in epilepsy, with particular reference to the temporal lobes*. Brain, 1966. **89**(3): p. 499-530.
84. Sloviter, R.S., *The neurobiology of temporal lobe epilepsy: too much information, not enough knowledge*. C R Biol, 2005. **328**(2): p. 143-53.
85. Ben-Ari, Y., et al., *The role of epileptic activity in hippocampal and "remote" cerebral lesions induced by kainic acid*. Brain Res, 1980. **191**(1): p. 79-97.
86. White, H.S., *Animal models of epileptogenesis*. Neurology, 2002. **59**(9 Suppl 5): p. S7-S14.
87. Turski, W.A., et al., *Seizures produced by pilocarpine in mice: a behavioral, electroencephalographic and morphological analysis*. Brain Res, 1984. **321**(2): p. 237-53.
88. Arida, R.M., et al., *The course of untreated seizures in the pilocarpine model of epilepsy*. Epilepsy Res, 1999. **34**(2-3): p. 99-107.
89. Mello, L.E., et al., *Circuit mechanisms of seizures in the pilocarpine model of chronic epilepsy: cell loss and mossy fiber sprouting*. Epilepsia, 1993. **34**(6): p. 985-95.
90. Lajko, N., et al., *Sensitivity of Rodent Microglia to Kynurenines in Models of Epilepsy and Inflammation In Vivo and In Vitro: Microglia Activation is Inhibited by Kynurenic Acid and the Synthetic Analogue SZR104*. Int J Mol Sci, 2020. **21**(23).
91. Zombori, T., *Animal experiments investigating epilepsy*, in *Department of Anatomy, Histology and Embriology*. 2012, University of Szeged: Szeged. p. 1-47.
92. Vezzani, A., B. Lang, and E. Aronica, *Immunity and Inflammation in Epilepsy*. Cold Spring Harb Perspect Med, 2015. **6**(2): p. a022699.
93. Thom, M., *Review: Hippocampal sclerosis in epilepsy: a neuropathology review*. Neuropathol Appl Neurobiol, 2014. **40**(5): p. 520-43.
94. Dobo, E., et al., *Interstrain differences of ionotropic glutamate receptor subunits in the hippocampus and induction of hippocampal sclerosis with pilocarpine in mice*. J Chem Neuroanat, 2015. **64-65**: p. 1-11.
95. Scarr, E., et al., *The distribution of muscarinic M1 receptors in the human hippocampus*. J Chem Neuroanat, 2016. **77**: p. 187-192.
96. Smolders, I., et al., *NMDA receptor-mediated pilocarpine-induced seizures: characterization in freely moving rats by microdialysis*. Br J Pharmacol, 1997. **121**(6): p. 1171-9.
97. Kienzler-Norwood, F., et al., *A novel animal model of acquired human temporal lobe epilepsy based on the simultaneous administration of kainic acid and lorazepam*. Epilepsia, 2017. **58**(2): p. 222-230.
98. Karoly, N., E. Dobo, and A. Mihaly, *Comparative immunohistochemical study of the effects of pilocarpine on the mossy cells, mossy fibres and inhibitory neurones in murine dentate gyrus*. Acta Neurobiol Exp (Wars), 2015. **75**(2): p. 220-37.
99. Mihaly, A., *The Reactive Plasticity of Hippocampal Ionotropic Glutamate Receptors in Animal Epilepsies*. Int J Mol Sci, 2019. **20**(5).
100. Wang, X., et al., *Persistent Hyperactivity of Hippocampal Dentate Interneurons After a Silent Period in the Rat Pilocarpine Model of Epilepsy*. Front Cell Neurosci, 2016. **10**: p. 94.
101. Magloczky, Z. and T.F. Freund, *Impaired and repaired inhibitory circuits in the epileptic human hippocampus*. Trends Neurosci, 2005. **28**(6): p. 334-40.

102. Sloviter, R.S., *"Epileptic" brain damage in rats induced by sustained electrical stimulation of the perforant path. I. Acute electrophysiological and light microscopic studies.* Brain Res Bull, 1983. **10**(5): p. 675-97.
103. Weiczner, R., B. Krisztin-Peva, and A. Mihaly, *Blockade of AMPA-receptors attenuates 4-aminopyridine seizures, decreases the activation of inhibitory neurons but is ineffective against seizure-related astrocytic swelling.* Epilepsy Res, 2008. **78**(1): p. 22-32.
104. Schidlitzki, A., et al., *A combination of NMDA and AMPA receptor antagonists retards granule cell dispersion and epileptogenesis in a model of acquired epilepsy.* Sci Rep, 2017. **7**(1): p. 12191.
105. Mihaly, A., K. Bencsik, and A. Nogradi, *Pharmacological inhibition of brain carbonic anhydrase protects against 4-aminopyridine seizures.* Acta Physiol Hung, 1994. **82**(2): p. 99-108.
106. Borbely, S., et al., *Modification of ionotropic glutamate receptor-mediated processes in the rat hippocampus following repeated, brief seizures.* Neuroscience, 2009. **159**(1): p. 358-68.
107. Buckmaster, P.S. and F.E. Dudek, *Neuron loss, granule cell axon reorganization, and functional changes in the dentate gyrus of epileptic kainate-treated rats.* J Comp Neurol, 1997. **385**(3): p. 385-404.
108. Karoly, N., A. Mihaly, and E. Dobo, *Comparative immunohistochemistry of synaptic markers in the rodent hippocampus in pilocarpine epilepsy.* Acta Histochem, 2011. **113**(6): p. 656-62.
109. Rigau, V., et al., *Angiogenesis is associated with blood-brain barrier permeability in temporal lobe epilepsy.* Brain, 2007. **130**(Pt 7): p. 1942-56.
110. Shin, C. and J.O. McNamara, *Mechanism of epilepsy.* Annu Rev Med, 1994. **45**: p. 379-89.
111. Sloviter, R.S., *The functional organization of the hippocampal dentate gyrus and its relevance to the pathogenesis of temporal lobe epilepsy.* Ann Neurol, 1994. **35**(6): p. 640-54.
112. Ribak, C.E., et al., *Inhibitory, GABAergic nerve terminals decrease at sites of focal epilepsy.* Science, 1979. **205**(4402): p. 211-4.
113. Rzezak, P., et al., *Everyday memory impairment in patients with temporal lobe epilepsy caused by hippocampal sclerosis.* Epilepsy Behav, 2017. **69**: p. 31-36.
114. Harrison, F.E., et al., *Spatial and nonspatial escape strategies in the Barnes maze.* Learn Mem, 2006. **13**(6): p. 809-19.
115. Vorhees, C.V. and M.T. Williams, *Assessing spatial learning and memory in rodents.* ILAR J, 2014. **55**(2): p. 310-32.
116. Barnes, C.A., *Memory deficits associated with senescence: a neurophysiological and behavioral study in the rat.* J Comp Physiol Psychol, 1979. **93**(1): p. 74-104.
117. Harrison, F.E., A.H. Hosseini, and M.P. McDonald, *Endogenous anxiety and stress responses in water maze and Barnes maze spatial memory tasks.* Behav Brain Res, 2009. **198**(1): p. 247-51.
118. Rodriguez Peris, L., et al., *Barnes maze test for spatial memory: A new, sensitive scoring system for mouse search strategies.* Behav Brain Res, 2024. **458**: p. 114730.
119. Mihaly, A., et al., *Neocortical cytopathology in focal aminopyridine seizures as related to the intracortical diffusion of [3H] 4-aminopyridine. Electrophysiologic and light-microscopic studies.* Acta Neuropathol, 1985. **66**(2): p. 145-54.
120. Mihaly, A. and B. Bozoky, *Immunohistochemical localization of extravasated serum albumin in the hippocampus of human subjects with partial and generalized epilepsies and epileptiform convulsions.* Acta Neuropathol, 1984. **65**(1): p. 25-34.

121. Farkas, I.G., et al., *Beta-amyloid peptide-induced blood-brain barrier disruption facilitates T-cell entry into the rat brain*. Acta Histochem, 2003. **105**(2): p. 115-25.
122. Gorter, J.A., E.A. van Vliet, and E. Aronica, *Status epilepticus, blood-brain barrier disruption, inflammation, and epileptogenesis*. Epilepsy Behav, 2015. **49**: p. 13-6.
123. Biernacki, T., et al., *Kynurenines in the Pathogenesis of Multiple Sclerosis: Therapeutic Perspectives*. Cells, 2020. **9**(6).
124. Vecsei, L., et al., *Kynurenines in the CNS: recent advances and new questions*. Nat Rev Drug Discov, 2013. **12**(1): p. 64-82.
125. Fulop, F., et al., *Syntheses, transformations and pharmaceutical applications of kynurenic acid derivatives*. Curr Med Chem, 2009. **16**(36): p. 4828-42.
126. Demeter, I., et al., *A novel kynurenic acid analog (SZR104) inhibits pentylenetetrazole-induced epileptiform seizures. An electrophysiological study : special issue related to kynurenine*. J Neural Transm (Vienna), 2012. **119**(2): p. 151-4.
127. Kovacs, A., et al., *Seizure, neurotransmitter release, and gene expression are closely related in the striatum of 4-aminopyridine-treated rats*. Epilepsy Res, 2003. **55**(1-2): p. 117-29.
128. Routy, J.P., et al., *The Kynurenine Pathway Is a Double-Edged Sword in Immune-Privileged Sites and in Cancer: Implications for Immunotherapy*. Int J Tryptophan Res, 2016. **9**: p. 67-77.
129. Kreutzberg, G.W., *Microglia: a sensor for pathological events in the CNS*. Trends Neurosci, 1996. **19**(8): p. 312-8.
130. Priller, J. and M. Prinz, *Targeting microglia in brain disorders*. Science, 2019. **365**(6448): p. 32-33.
131. Hickman, S., et al., *Microglia in neurodegeneration*. Nat Neurosci, 2018. **21**(10): p. 1359-1369.
132. Deczkowska, A., et al., *Disease-Associated Microglia: A Universal Immune Sensor of Neurodegeneration*. Cell, 2018. **173**(5): p. 1073-1081.
133. Belov Kirdajova, D., et al., *Ischemia-Triggered Glutamate Excitotoxicity From the Perspective of Glial Cells*. Front Cell Neurosci, 2020. **14**: p. 51.
134. Pocock, J.M. and H. Kettenmann, *Neurotransmitter receptors on microglia*. Trends Neurosci, 2007. **30**(10): p. 527-35.
135. Hovens, I.B.N., C.; Shoemaker, R.G., *A novel method for evaluating microglial activation using ionized calcium-binding adaptor protein-1 staining: Cell body to cell size ratio*. Neuroimmunol. Neuroinflamm., 2014. **1**: p. 82-88.
136. Biróné, N.L., *Kynurenic acid and its analog SZR104 exhibit strong antiinflammatory effects and alter the intracellular distribution and methylation patterns of H3 histones in immunochallenged microglia-enriched cultures of newborn rat brains*, in *Department of Cell Biology and Molecular Medicine, Albert Szent-Györgyi Medical School – Faculty of Science and Informatics*. 2022, University of Szeged, Hungary: Szeged. p. 22-34.
137. George Paxinos, K.B.J.F., *The Mouse Brain in Stereotaxic Coordinates*. 1997, San Diego, CA, USA: Academic Press.
138. Reyes, A., et al., *Impaired spatial pattern separation performance in temporal lobe epilepsy is associated with visuospatial memory deficits and hippocampal volume loss*. Neuropsychologia, 2018. **111**: p. 209-215.
139. Pitts, M.W., *Barnes Maze Procedure for Spatial Learning and Memory in Mice*. Bio Protoc, 2018. **8**(5).
140. Khaksooy, A.M.C., F., *Practical Biostatistics in Translational Healthcare*. 2018, Berlin/ Heidelberg, Germany: Springer.

141. He, D.F., et al., *Morpho-physiologic characteristics of dorsal subicular network in mice after pilocarpine-induced status epilepticus*. Brain Pathol, 2010. **20**(1): p. 80-95.
142. Volz, F., et al., *Stereologic estimation of hippocampal GluR2/3- and calretinin-immunoreactive hilar neurons (presumptive mossy cells) in two mouse models of temporal lobe epilepsy*. Epilepsia, 2011. **52**(9): p. 1579-89.
143. Kettenmann, H., et al., *Physiology of microglia*. Physiol Rev, 2011. **91**(2): p. 461-553.
144. Van Den Herrewegen, Y., et al., *The Barnes Maze Task Reveals Specific Impairment of Spatial Learning Strategy in the Intrahippocampal Kainic Acid Model for Temporal Lobe Epilepsy*. Neurochem Res, 2019. **44**(3): p. 600-608.
145. Hauser, J., et al., *Small lesions of the dorsal or ventral hippocampus subregions are associated with distinct impairments in working memory and reference memory retrieval, and combining them attenuates the acquisition rate of spatial reference memory*. Hippocampus, 2020. **30**(9): p. 938-957.
146. Kopniczky, Z., et al., *Alterations of behavior and spatial learning after unilateral entorhinal ablation of rats*. Life Sci, 2006. **78**(23): p. 2683-8.
147. Muller, C.J., et al., *Behavioral and cognitive alterations, spontaneous seizures, and neuropathology developing after a pilocarpine-induced status epilepticus in C57BL/6 mice*. Exp Neurol, 2009. **219**(1): p. 284-97.
148. Choi, D.W., *Glutamate neurotoxicity and diseases of the nervous system*. Neuron, 1988. **1**(8): p. 623-34.
149. Seitelberger, F., H. Lassmann, and O. Hornykiewicz, *Some mechanisms of brain edema studied in a kainic acid model*. Acta Neurobiol Exp (Wars), 1990. **50**(4-5): p. 263-7.
150. Rasmussen, H., *The calcium messenger system (I)*. N Engl J Med, 1986. **314**(17): p. 1094-101.
151. Olney, J.W., *Excitotoxicity: an overview*. Can Dis Wkly Rep, 1990. **16 Suppl 1E**: p. 47-57; discussion 57-8.
152. Olney, J.W., *Excitatory transmitters and epilepsy-related brain damage*. Int Rev Neurobiol, 1985. **27**: p. 337-62.
153. Walker, M.C., *Pathophysiology of status epilepticus*. Neurosci Lett, 2018. **667**: p. 84-91.
154. Honavar, M., Meldrum, B.S., *Epilepsy*, in *Greenfield's Neuropathology*, P.I. Graham, Lantos, P.L., Editor. 2002, Arnold: London, UK. p. 899-941.
155. Tai, X.Y.B., B.; Thom, M.; Thompson, P.; Baxendale, S.; Koeppe, M.; Bernasconi, N., *Neurodegenerative processes in temporal lobe epilepsy with hippocampal sclerosis: Clinical, pathological and neuroimaging evidence*. Neuropathol. Appl. Neurobiol., 2017(44): p. 70-90.
156. Rizzi, M., et al., *Glia activation and cytokine increase in rat hippocampus by kainic acid-induced status epilepticus during postnatal development*. Neurobiol Dis, 2003. **14**(3): p. 494-503.
157. Borges, K., et al., *Neuronal and glial pathological changes during epileptogenesis in the mouse pilocarpine model*. Exp Neurol, 2003. **182**(1): p. 21-34.
158. Kang, T.C., et al., *Epileptogenic roles of astroglial death and regeneration in the dentate gyrus of experimental temporal lobe epilepsy*. Glia, 2006. **54**(4): p. 258-71.
159. Wang, C., et al., *Microglia mediate forgetting via complement-dependent synaptic elimination*. Science, 2020. **367**(6478): p. 688-694.
160. Buckmaster, P.S., *Mossy Fiber Sprouting in the Dentate Gyrus*, in *Jasper's Basic Mechanisms of the Epilepsies*, J.L. Noebels, et al., Editors. 2012: Bethesda (MD).
161. Thorn, M.M., L.; Catarino, C.; Yogarajah, M.; Koeppe, M.J.; CABoclo, L.; Sisodiya, S.M., *Bilateral reorganization of the dentate gyrus in hippocampal sclerosis: A postmortem study*. Neurology, 2009(73): p. 1033-1040.

162. Lurton, D. and E.A. Cavalheiro, *Neuropeptide-Y immunoreactivity in the pilocarpine model of temporal lobe epilepsy*. Exp Brain Res, 1997. **116**(1): p. 186-90.
163. Wu, Y.F. and S.B. Li, *Neuropeptide Y expression in mouse hippocampus and its role in neuronal excitotoxicity*. Acta Pharmacol Sin, 2005. **26**(1): p. 63-8.
164. Nadler, J.V., et al., *Neuropeptide Y in the recurrent mossy fiber pathway*. Peptides, 2007. **28**(2): p. 357-64.
165. Papp, P., et al., *Alterations in hippocampal and cortical densities of functionally different interneurons in rat models of absence epilepsy*. Epilepsy Res, 2018. **145**: p. 40-50.
166. Botterill, J.J., et al., *Selective plasticity of hippocampal GABAergic interneuron populations following kindling of different brain regions*. J Comp Neurol, 2017. **525**(2): p. 389-406.
167. Cameron, S., et al., *Proportional loss of parvalbumin-immunoreactive synaptic boutons and granule cells from the hippocampus of sea lions with temporal lobe epilepsy*. J Comp Neurol, 2019. **527**(14): p. 2341-2355.
168. Filice, F., et al., *Parvalbumin-expressing ependymal cells in rostral lateral ventricle wall adhesions contribute to aging-related ventricle stenosis in mice*. J Comp Neurol, 2017. **525**(15): p. 3266-3285.
169. Lichvarova, L., et al., *Parvalbumin expression in oligodendrocyte-like CG4 cells causes a reduction in mitochondrial volume, attenuation in reactive oxygen species production and a decrease in cell processes' length and branching*. Sci Rep, 2019. **9**(1): p. 10603.
170. Martin Dokter, O.v.B.u.H., *Neurogenesis within the adult hippocampus under physiological conditions and in depression*. Neural. Regen. Res., 2012(5;7(7)): p. 552-9.
171. Kempermann, G., H. Song, and F.H. Gage, *Adult neurogenesis in the hippocampus*. Hippocampus, 2023. **33**(4): p. 269-270.
172. Toth, K., et al., *Loss and reorganization of calretinin-containing interneurons in the epileptic human hippocampus*. Brain, 2010. **133**(9): p. 2763-77.
173. Blumcke, I., et al., *Preservation of calretinin-immunoreactive neurons in the hippocampus of epilepsy patients with Ammon's horn sclerosis*. J Neuropathol Exp Neurol, 1996. **55**(3): p. 329-41.
174. Blumcke, I., et al., *An increase of hippocampal calretinin-immunoreactive neurons correlates with early febrile seizures in temporal lobe epilepsy*. Acta Neuropathol, 1999. **97**(1): p. 31-9.
175. Lee, M., *Neurotransmitters and microglial-mediated neuroinflammation*. Curr Protein Pept Sci, 2013. **14**(1): p. 21-32.
176. Benson, M.J., S. Manzanero, and K. Borges, *Complex alterations in microglial M1/M2 markers during the development of epilepsy in two mouse models*. Epilepsia, 2015. **56**(6): p. 895-905.
177. Kawabori, M. and M.A. Yenari, *The role of the microglia in acute CNS injury*. Metab Brain Dis, 2015. **30**(2): p. 381-92.